RADIOACTIVE TRACER DETERMINATION OF GASEOUS DIFFUSION COEFFICIENTS

by

THOMAS ERIC MISTLER

B. S., Kansas State University, 1963

A MASTER'S THESIS

submitted in partial fulfillment of the

requirements for the degree

MASTER OF SCIENCE

Department of Nuclear Engineering

KANSAS STATE UNIVERSITY
Manhattan, Kansas

1966

Approved by:

John O. Mingle

Major Professor

TABLE OF CONTENTS

TABLE OF CONTENTS (continued)

LIST OF TABLES

LIST OF FIGURES

NOMENCLATURE

C	Concentration of tagged material at z
C_o	Concentration of tagged material at zero time
c	Number of constraints
D	Coefficient of diffusion
D_e	Effective diffusion coefficient (refers to diffusion in transition range)
$D_{e_{12}}$	Effective experimental D for $C^{14}O_2$ in CO_2
D_k	Coefficient of Knudsen diffusion
D_{11}	Self-diffusion coefficient
D_{12}	Mutual diffusion coefficient for species 1 and 2
F	Flow rate in moles
f_D	First two terms of a Taylor's series expansion for the partial of Re with respect to D
$f_i(r,v_i,t)$	Distribution function
G	Hydrodynamic molecular flow
F	Half-length of capillary tube
$\overline{J}$	Mean molecular flow per unit area per unit time
j_{iz}	Molecular flux in direction z
K_n	Knudsen number, (ℓ/r)
K_o	Representative Knudsen length for porous medium
k	Boltzmann constant for a molecule
L	Effective length of capillary tube
$\mathcal{L}[f(t)]$	Laplace transform of f(t)
$\mathcal{L}^{-1}[f(s)]$	Inverse Laplace transform of f(s)
ℓ	Mean free path length

m	Molecular mass
m_i	Molecular mass of species i
N	Number of data points
N^*	Molecular transport in molecules per unit time
$(N-c)$	Number of degrees of freedom associated with σ_x^2
n	Number of molecules per unit volume
p	Pressure
p^*	Porosity factor
q	Tortuosity factor
R	Radius of capillary tube used in experiment
R^*	Gas constant per gram
Re	Residue
r	Radius of capillary tube
s	Laplacian variable
T	Absolute temperature
T^*	Temperature dependent potential energy parameter for i-j interaction, (ϵ_{ij}/k)
t	Time
U_o	Slip velocity of gas at tube wall
V_1	Volume of tagged reservoir
V_2	Volume of untagged reservoir
$\bar{v}$	Arithmetic mean speed
Xc_i	Calculated value of X at time i
Xe_i	Experimental value of X at time i
$X(\tau,\xi)$	Dimensionless concentration gradient, (C/C_o)
Y_{1a}, Y_{1b}	Mole fractions of species 1 at each end of the diffusion path

z	Distance variable along tube
α	Dimensionless parameter for volume of tagged reservoir, $(\pi R^2 L/V_1)$
β	Dimensionless parameter for volume of untagged reservoir, $(\pi R^2 L/V_2)$
γ	Euler's constant
ϵ_{ij}	Force constant for i-j interaction
η	Viscosity
λ_n	Eigenvalues of transcendental equation
ξ	Dimensionless distance variable, (z/L)
ρ	Density
σ	Molecular diameter
σ_D	Standard deviation for D obtained by least squares analysis
σ_D^2	Variance of calculated D value
σ_i	Molecular diameter of species i
σ_x	Standard deviation of least squares calculation of $X(\tau,\xi)$
σ_x^2	Variance of $X(\tau,\xi)$ calculation by least squares analysis
σ_{12}	Effective diameter of 1-2 interaction
τ	Dimensionless time variable, (tD/L^2)
Ω_{ij}	Potential energy parameter for i-j interaction

1.0 INTRODUCTION AND THE THEORY OF DIFFUSION

1.1 Ordinary Gaseous Diffusion

The phenomena of diffusion, viscosity, and thermal conductivity are physically similar in that they involve the transport of mass, momentum and energy, respectively. By using a simplified kinetic theory which involves making many simplifying assumptions throughout, it is, nevertheless, possible to obtain expressions which describe the primary dependence of these transport coefficients upon the temperature, pressure, mass, and size of the molecules in the gas. While the procedure for evaluating the coefficients of diffusion, viscosity, and thermal conductivity are quite similar, only the former will be considered in this paper.

The simplified kinetic theory of gases (42) is based upon the following three assumptions which provide a simple model for a gas containing n molecules per unit volume:

(i) The molecules are rigid, non-attracting spheres with diameter σ.

(ii) All the molecules travel with the same speed; the usual choice for the molecular speed is the arithmetic mean speed, $\bar{v} = (8kT/m\pi)^{1/2}$, calculated from the velocity distribution function.

(iii) All the molecules travel in a direction parallel to one of the coordinate axes.

Since, by assumption (i), the gas described by this model is composed of impenetrable elastic spheres it is possible to introduce a quantity known as the mean free path. The mean free path is the average distance traversed by a molecule between collisions. By examining the dependence of the rate of collisions upon the size, number density, and average speed of the molecules

and using $p = nkT$ from the ideal gas law, the mean free path length, ℓ, can be shown to be (29)

$$\ell = kT/(\sqrt{2}p\sigma^2). \tag{1}$$

For simple molecules, σ is about 3×10^{-8} cm and at one atmosphere pressure and 20°C the mean free path of a gas molecule is given as $\ell \approx 10^{-5}/p$ cm where p is in atmospheres. On the basis of this simple kinetic theory the diffusion coefficient can be expressed in terms of the quantity ℓ. By utilizing a more rigorous approach to kinetic theory, the mean free path length does not, however, appear directly in the derivation of the diffusion coefficient.

The coefficient of diffusion, D, is the flux of molecules of a particular species, due to a gradient in the number density of the molecules of that species. The number density gradient may be caused by concentration, pressure, and in some instances temperature gradients. For a fast one dimensional approach, the mean free path length concept suggested previously is utilized in determining j_{iz}, the number of type i molecules moving in direction z, crossing a perpendicular plane per unit area per unit time. This approach yields the following relationship:

$$j_{iz} = -(1/3)\ \bar{v}\ell\ \frac{dn_i}{dz} \tag{2}$$

where $\bar{v}$ is the arithmetic mean speed. The diffusion coefficient, which is accurately described as a self-diffusion coefficient when only one type of gas is present, is defined in terms of the flux as follows:

$$j_{iz} = -D\ \frac{dn_i}{dz}\ . \tag{3}$$

A comparison of Eqs. (2) and (3) yields

$$D = (1/3)\ \bar{v}\ell = (2/3)\ (\pi mkT)^{1/2}/\pi\sigma^2\rho \tag{4}$$

where $\rho = nm = pm/kT$ is the density of the gas.

The expression for the diffusion coefficient is found from considerations of rigorous kinetic theory for rigid sphere molecules to have the same general form as Eq. (3) above. This more rigorous theory predicts however, that the constant multiplier to the right hand side of Eq. (4) should be 3/8 instead of 2/3. Inserting this value into Eq. (4) produces

$$D = 2.6280 \times 10^{-3} (T^3/m)^{1/2}/p\sigma^2, \text{ cm}^2/\text{sec} \qquad (5)$$

where m = molecular weight,

T = temperature in ^{o}K,

p = pressure in atmospheres,

σ = molecular diameter in Å.

For a mixture of two species of gases the coefficient of diffusion, D_{12}, for the same rigid sphere model, according to Chapman (16) is

$$D_{12} = 2.6280 \times 10^{-3} (T^3(m_1+m_2)/2m_1m_2)^{1/2}/p\sigma_{12}^2, \text{ cm}^2/\text{sec} \qquad (6)$$

for which $\sigma_{12} = 1/2(\sigma_1+\sigma_2)$.

Although Eqs. (5) and (6) are sufficiently accurate for some considerations they do not show the proper relationship for the diffusion coefficient as a function of temperature and pressure. For an accurate description of the diffusion coefficient as a function of pressure and temperature it is necessary to incorporate in the model the effect of the interactions which take place between real molecules. It is convenient to use the potential energy of interaction to mathematically describe the physical interaction of real molecules. Several such potential energy functions have been developed for polar and non-polar molecules coupling the attractive long range forces to the short range repulsive forces which exist between real molecules. According to Hirschfelder (42), the Lennard-Jones potential energy function

and the Stockmayer potential are reasonably accurate for polar and non-polar molecules, respectively. It is necessary to go to a detailed classical treatment of the rigorous theory of dilute monatomic gases and mixtures to successfully describe the dependence of diffusion coefficients on the potential energy function of molecular interaction.

A knowledge of the distribution function $f_i(r,v_i,t)$ is the basis for the rigorous development of the kinetic theory of gases. This function represents the number of molecules of the i^{th} species which lie in a unit volume element about the point r at time t and which have velocities within a unit range about v_i. If there are no gradients in the gas the distribution $f_i(r,v_i,t)$ reduces to the Maxwellian distribution. When the gaseous system is not at equilibrium, the distribution must satisfy the Boltzmann integro-differential equation. If the condition of a gas is only slightly different from equilibrium, then the distribution function is nearly Maxwellian and the Boltzmann equation can be solved by the perturbation method of Chapman and Enskog (16). The solution to the Boltzmann equation can then be used to obtain expressions for mass flux and diffusion coefficients. These expressions show that in addition to the concentration gradient, as shown by simple kinetic theory, the temperature gradient as a second order effect causes mass transfer as well. Neglecting temperature effects, the first approximation to the coefficient of diffusion of a binary mixture obtained from the Chapman-Enskog theory is

$$D_{12} = 0.002628(T^3(m_1+m_2)/2m_1m_2)^{1/2}/p\sigma_{12}^2\Omega_{12}T_{12}^* \qquad (7)$$

where D_{12} = diffusion coefficient in cm^2/sec,

p = pressure in atmospheres,

T = temperature in ^oK,

$T^*_{12} = kT/\epsilon_{12}$,

$m_1 m_2$ = molecular weights of species 1 and 2, respectively,

σ_{12}, ϵ_{12}/k = molecular potential energy parameters characteristic of 1-2 interaction in Å and °K, respectively,

Ω_{12} = a complicated potential energy parameter which indicates the deviation of any particular molecular model from the idealized rigid-sphere model (42).

When Eq. (7) is written for a single component, the coefficient of self-diffusion is obtained:

$$D_{11} = 0.002628(T^3/m)^{1/2}/p\sigma_{11}^2\Omega_{11}T_{11}^* \qquad (8)$$

where D_{11} = coefficient of self diffusion in cm^2/sec and the other parameters are the same as for Eq. (7). It should be noted that D_{12} is inversely proportional to p, so that as the pressure is decreased, the diffusion coefficient is increased. Also, the diffusion coefficient is approximately proportional to $(T)^{3/2}$ so that for a particular gas at a constant pressure, D_{12} is clearly dependent upon the temperature of the gas. Other formulae for the calculation of diffusion coefficients in the moderate pressure or bulk flow range are available in the literature (16,17,21,42). The Chapman-Enskog kinetic theory Eq. (7) has been widely adopted for moderate pressures and is considered adequate for this study.

The Chapman-Enskog kinetic theory of gases produces results which are limited in applicability to some extent by the underlying assumptions of the theory. The consideration of only binary collisions causes the theory to be inapplicable at high pressures where three body collisions are of importance. The application of the theory to low temperature processes where quantum mechanical considerations must be made is excluded by the use of classical

mechanics in the development of the theory. The first solution to the Boltzmann equation by the Chapman-Enskog method (16), which provides a series approximation to the distribution function, is valid only when relative changes in concentration, velocity, and temperature are much less than unity across a length of one mean free path in the gaseous medium (that is, $\ell(\partial \ln n/\partial z)<<1$). The mean free path in a gas at greater than one atmosphere pressure is less than 10^{-5}cm; consequently, at pressures greater than one atmosphere it is only under conditions of extreme gradients that this assumption is unrealistic. On the other hand, since the mean free path length varies inversely with pressure, the theory loses its applicability at low pressures when only slight gradients exist. Finally, the assumption that the dimensions of the constraints to the gaseous system are large compared to the mean free path length causes the reliability of the theory to be lost for flow conditions in rarefied gases. Because this study is concerned primarily with mass transport of rarefied gases it is appropriate to consider this difficulty in greater detail.

1.2 Knudsen Diffusion

Free-molecule or Knudsen flow occurs in the pressure region in which the mean free path ℓ of the molecules is many times greater than the characteristic dimension of any surface moving through the gas (14). The number of collisions between molecules in the gas is negligible in comparison with the number of collisions between gas molecules and the surface; hence, there is little mechanism for the establishment of local equilibrium. Such free-molecule or Knudsen flow is really a process of diffusion, and takes place for each constituent of a mixture along its own partial pressure or concentration gradient. The characteristics of ideal Knudsen flow are reasonably

well understood (63).

Several attempts have been made to describe accurately and theoretically the behavior of gases in the transition range, (that density region between a Knudsen gas and a moderately dense gas where Poiseuille or bulk flow occurs). Although several theoretical treatments presented for this transition range are convincing (27,30,65,70,73), no single treatment has been universally accepted. Experimental data for the transition range are extremely scarce (32); hence, any rigorous or empirical equations for transport coefficients in the transition range have not been tested with convincing experimental data.

Having discussed ordinary gaseous diffusion and described the problem of gaseous diffusion in the transition range, it is appropriate to consider the detail of Knudsen diffusion before proceeding to a survey of formulae for diffusion in the transition pressure range. Knudsen diffusion results in the flow or diffusion of gases through a capillary tube of radius r or porous solid where the diameter of the tube or pore becomes much less than ℓ, the molecular mean free path. Qualitatively, this flow region appears to occur when the Knudsen number K_n, which equals ℓ/r, is greater than 10 (28). At small pore diameters diffusion or flow is impeded by impact with pore surfaces rather than by molecular interaction which causes the development of collective flow behavior. Because the mean free path length is much greater than r, it is possible to neglect intermolecular collisions. Since the molecular flow is determined by collisions with the wall, the effect of such a molecule-wall collision on the direction of movement of the molecule must be investigated (25).

A specular reflection of a molecule colliding with the wall would only

occur if the wall were perfectly smooth on the submicroscopic scale. Even the condition of smoothness would not cause specular reflection if incident molecules adhered to the reflecting surface. It is not surprising, therefore, that the experiments of Knudsen on the nature of reflection of molecules from glass surfaces indicate almost 100 percent diffuse reflection (53,66).

If the actual irregular wall is replaced by a smooth mathematical surface which reflects incident molecules diffusely, the number of molecules reflected from a unit area of the wall per unit time in a particular direction is equal to the number crossing the unit area of the mathematical surface in that direction. This quantity is obtained by integrating over all the speeds of the molecules within some solid angle about the path of the molecule as it emerges from the mathematical wall. Using this expression for the distribution of the molecules moving in a set direction, the net molecular transport through a cross section of the tube can be calculated. The resulting formula for the net transport of molecules per unit time through the tube is (66)

$$N^* = -(2\pi r^3 \bar{v}/3) \frac{dn}{dz} \tag{9}$$

or converting to mean flow per unit area per unit time,

$$\bar{J} = -(2\bar{v}r/3) \frac{dn}{dz}. \tag{10}$$

An examination of Eq. (10) indicates that flow in a capillary tube is proportional to the density gradient and opposite in direction; hence, the flow has the characteristics of diffusion. The inferred Knudsen diffusion coefficient, $(2\bar{v}r/3)$, is quite similar to the bulk range diffusion coefficient, $(\bar{v}\ell/3)$, and, as one would expect, has the tube diameter appearing in place of the mean free path. It is noted that in Knudsen flow, the diffusion coefficient D_k is proportional to $T^{1/2}$, to the pore diameter, and is independent of the

total pressure. Using an assumed Maxwellian velocity distribution the result becomes

$$D_k = (2r/3)(8kT/\pi m)^{1/2}$$

$$= 9700r(T/m)^{1/2} cm^2/sec, \qquad (11)$$

where D_k = coefficient of Knudsen diffusion in cm^2/sec,

r = pore radius in cm,

m = molecular weight of the species,

T = absolute temperature in ^oK.

For carbon dioxide at 25^oC and at a pressure for which $K_n > 10$, D_k equals 1259 cm^2/sec for a pore diameter of 1 mm. For the diffusion of CO_2 in N_2 at 25^oC in a pore of radius 0.05 cm, D_k and D_{11} become the same at a pressure of 89.2 microns. For diffusion at one atmosphere pressure the coefficients are equal for a pore size of 588 Å.

If Knudsen flow of a binary gas mixture occurs, the component gases will diffuse along the tube independently and Eq. (9) can be applied to each gas separately if n is assumed to refer to one species of molecules in the mixture. For steady flow, N must be constant along the tube; therefore, the density gradient $\frac{dn}{dz}$ is uniform and can be replaced by $\Delta n/L$ where Δn is the difference in density between the ends and L is the tube length. Since $\Delta n = \Delta p/kT$ from Eq. (9), the flow rate in moles is

$$F(moles) = (D_k \pi r^2)\Delta p/LR^*T \qquad (12)$$

where F applies to the component with partial pressure drop Δp, and R^* is the gas constant per gram. It is noted that the flux of a particular component is inversely proportional to its molecular weight. These formulae for Knudsen flow have a sound theoretical basis and have been verified by experimental

work.

1.3 Transition Range Diffusion

In many chemical processes the diffusion of gas through capillaries or through the fine channels of porous solids is of considerable importance. As has been shown, the transport of gas through a small channel may occur in three ways. When the Knudsen number based upon the equivalent radius and mean free path is less than 0.1, i.e., $K_n < 0.1$, transport may take place because of Poiseuille flow if a pressure gradient exists, or by ordinary diffusion if a partial pressure gradient exists. When K_n is greater than 10 transport occurs by Knudsen flow in the presence of either a total or partial pressure gradient. When gas flow occurs in the transition range, i.e., $0.1 < K_n < 10$, the mechanism for diffusive transport must be a combination of intermolecular collisions, molecule-wall collisions, and the resultant viscous effects which cause a velocity profile in the tube. The flow of gases at ordinary temperatures and pressures through many commercial porous catalysts occurs in the intermediate or transition range. Also the frictional drag of rarefied gases upon ballistics (conditions prevalent when space capsules re-enter the atmosphere of the earth) is dependent in part upon the mechanism for gas flow in this transition range (71,76). Thus, today the problem of gas flow in the transition range holds special interest for theoreticians and experimentalists.

At the high pressure end of the transition range it is necessary to differentiate two distinct limiting forms of the gas transport through a tube. The two mechanisms are hydrodynamic viscous flow and gaseous diffusion. The hydrodynamic flow occurs only when a gradient in the total pressure exists. From the usual treatment of hydrodynamic flow of a viscous fluid in a long

cylindrical tube, the molecular flow G is given as (52)

$$G = n\bar{v}r^2(U_o - (r^2/8\eta)\frac{dp}{dz}) \tag{13}$$

where η is the viscosity, n the molecular density, and U_o the "slip" velocity at the tube wall. Using the values of η, p, and U_o, from simple kinetic theory, Eq. (13) may be written in the form

$$G = (\pi r^3/m\bar{v} + (3\pi r^3/8m\bar{v})r/\ell)\frac{dp}{dz}. \tag{14}$$

By Eq. (14) it is clear that the effect of "slip" at the tube wall increases the flow as the Knudsen number increases. In the low pressure limit, Eq. (14) reduces to the slip flow correction term (66) which has the same form as Knudsen flow but is smaller. If the specific flow is plotted versus mean pressure and the equation for Knudsen flow considered, it is possible to infer a minimum in the specific flow curve at low pressure.

The case of gaseous diffusion at the high pressure side of the transition regime occurs at uniform total pressure and represents transport due to random motion without drift. This transport due to interdiffusion of molecules can be given by the relation

$$G = -(\pi r^2 D_{12}/kT)\frac{dp_1}{dz} \tag{15}$$

where p_1 is the partial pressure of the species 1 and D_{12} is the diffusion coefficient of the gas. It is noted that Eq. (15) is essentially the same as Eq. (11) for Knudsen flow. As has been shown, the effective diffusion coefficient for the transition range D_e, appropriate to Eqs. (12) and (15) in the limiting cases, is dependent upon a diffusion process of mixed character. A summary of the results of existing treatments for D_e is given below.

Bosanquet (9) has given an additive resistance law

$$1/D_e = 1/D_k + 1/D_{12} \tag{16}$$

which states that the resistance to transport is the sum of the resistance caused by wall collisions and by intermolecular collisions. Bosanquet's additive resistance law was originally obtained by an elementary mean free path argument[1] but it appears to be in agreement with more sophisticated calculations (30,65) and with the limited experimental data available (29).

Wheeler (87) has proposed an empirical combination as

$$D_e = D_{12}\left[1-\exp(-D_k/D_{12})\right] \tag{17}$$

This equation has been deduced from intuitive reasoning but it does give a smooth transition between the two extremes. For the system CO_2 in N_2 at 25°C this effective diffusion coefficient is shown in Fig. 1 as a function of pressure for diffusion through a one millimeter tube. It is noted that in the range of three to three hundred microns of mercury pressure that these combination rules of Bosanquet and Wheeler disagree. This, in essence, comprises the transition range.

In another treatment based upon elementary momentum transport theory, Scott (73) has shown that a complicated log-mean expression involving the actual fluxes should be employed to define the effective diffusion coefficient as follows

$$D_e = D_{12}/X_{LM} \tag{18}$$

---

[1] Bosanquet (9) considers the diffusion process in the tube as a random walk process in which the succesive steps of the individual molecules are terminated either by collisions with other molecules or with the tube wall. The mean step size is then related to the mean free paths for wall collisions and gas collisions by taking the total collision frequency to be $\bar{v}/\ell$. Knowing that the frequencies of the two types of collisions are additive and that D_k and D_{12} can be taken proportional to $\bar{v}$ times the mean step size, the additive resistance law is derived.

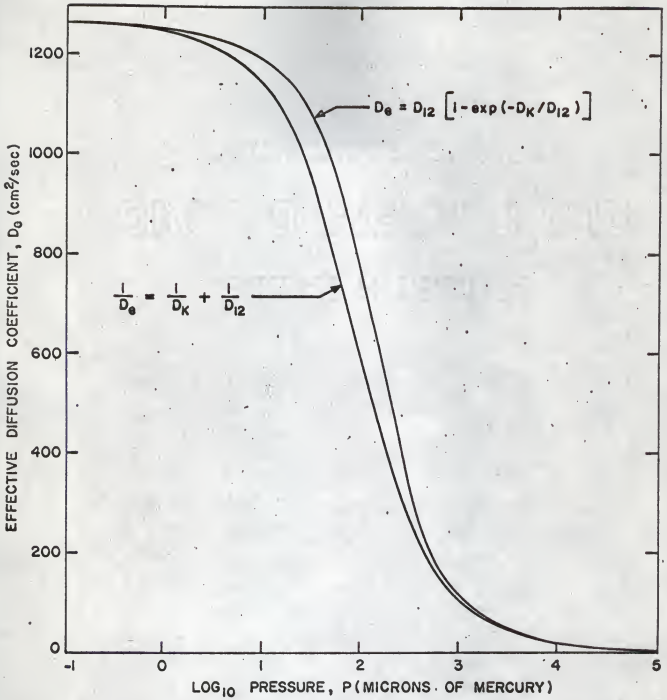

Fig. 1. Effective diffusion coefficient for CO_2 in a N_2 system at 25° C. with a 1.0 mm I.D. tube.

where $X_{LM} = \alpha(Y_{1a} - Y_{1b})/\ln(A_b/A_a)$,

$A_b = 1-\alpha Y_{1b} + D_{12}/D_k$,

$A_a = 1-\alpha Y_{1a} + D_{12}/D_k$,

$\alpha = 1 + N_1/N_2$,

Y_{1a}, Y_{1b} = mole fractions of species 1 at each end of the diffusion path,

N_1, N_2 = total rate of transport of species 1 and 2 in moles per unit time per unit area, respectively.

This expression reduces to the additive resistance law if the diffusion is countermolal. At the present time Scott's data are only for catalyst type materials where some averaging parameters are necessary for any application of the analysis.

Using the Stefan-Maxwell momentum balance method, Rothfeld (70) derived an equation for constant pressure binary diffusion through a porous medium equivalent to Eq. (18). He has presented data for five different binary gas systems (five different trace gases diffusing against helium) diffusing through porous cylindrical pellets which seem to fit his model. His data, like Scott's, require the use of some averaging parameters characteristic of the catalyst type material.

Evans (30) has derived a combining rule similar to Bosanquet's by applying the rigorous kinetic theory of multicomponent gases to his "dusty gas" model for gas molecules in a porous medium. In this model the porous medium is assumed to be a collection of stationary giant molecules through which the real gas molecules flow. The entire pressure range is covered by letting the mole fraction of real gas molecules vary between zero and one. The relationship given is

$$1/D_e = 1/(D_{12})_{eff} + 1/(D_{1k})_{eff} \tag{19}$$

where $(D_{12})_{eff} = p^* D_{12}/q$

$(D_{1k})_{eff} = 2K_o D_k/r.$

Here p^* is the porosity and q the tortuosity factor for the medium while K_o is a representative Knudsen length for the medium. These quantities must be obtained by experiment for a particular medium. Evans (29) also has a limited amount of data to support his model.

The effect of tube length on the diffusion coefficient has been considered by Pollard and Present (65) in their treatment of gaseous self-diffusion in long capillary tubes. The diffusion coefficient in the Knudsen limit is shown by involved formulae to be smaller for a tube of finite length than for an infinite tube by the factor (1-3r/8L). It is shown that the diffusion coefficient in all tubes longer than a given value L should be the same at pressures for which $\ell < H$, where H is the half-length of the tube. For a tube of infinite length D_e is given as

$$D_e = (\bar{v}\ell/3)\left[1 - 3\ell/8r + (6\ell/\pi r)Q(r/\ell)\right] \tag{20}$$

where $Q(r/\ell) = \pi/3(3/16 - r/2\ell + r^2/\ell^2 - r^3 I/\ell^3)$,

$I = 1.2264 - (3/4)\ln(2\gamma r/\ell)$,

γ = Euler's constant.

For the two limiting cases for an infinite tube:

(a) Knudsen range ($\ell >> r$)

$$D_e = (2\bar{v}r/3)(1 - rI/\ell) + \ldots \tag{21}$$

(b) bulk range ($\ell << r$)

$$D_e = (\bar{v}\ell/3)(1 - 3\ell/8r). \tag{22}$$

Eqs. (21) and (22) are in agreement with Eqs. (11) and (4) respectively. For a tube of finite length at a pressure for which $\ell >> H >> r$, D_e is given as

$$D_e = (3\bar{v}r/8)(1-3r/4H - (r/\ell)(0.4764 + 0.75 \ln(H/2r)). \qquad (23)$$

A very close agreement has been shown to exist between these relations for D_e and the additive resistance law of Bosanquet.

DeMarcus (24) has computed some flow amounts under various conditions of roughness for pore walls. He does not give an expression for the effective diffusion caused by a combination of the two asymptotic flow mechanisms.

Wakao, Otani, and Smith (85) have derived equations for the effect of simultaneous total pressure and concentration gradients which apply in Knudsen number ranges from Knudsen to Poiseuille flow. Knudsen's original data for CO_2 and new measurements on nitrogen in a glass capillary are in close agreement with the equations presented. This account does not, however, give any new information concerning the effective diffusion coefficient for constant total pressure in the transition range.

It is the purpose of the present study to examine an experimental method which can be used to determine the effective diffusion coefficients for various binary mixtures in this transition range.

2.0 EXPERIMENTAL THEORY

2.1 Introduction

In order to measure diffusion coefficients it becomes necessary to establish a concentration gradient for the desired component. Generally two methods are applied to bring about this result: (I) a steady-state type of experiment in which flow streams of different compositions pass on opposite sides of a barrier through which diffusion occurs, or (II) a transient experiment whereby diffusion eliminates a zero-time concentration difference between two parts of a closed batch system. Method (I) requires a large amount of material as well as precise flow control and is losing some of its popularity to Method (II). Early measurements by Method (I) were made by Buckingham (13) on porous soil; more recent measurements on catalysts and adsorbents include those of Scott and Dullien (73), Otani and coworkers (62), Evans and coworkers (30), and Wakao and Smith (84). The difficulty with Method II has been the measurement of the concentration as a function of time, but the advances of radioisotope detection and availability have made their use very feasible for this type of experiment. In particular, the recent development of semiconductor radiation detectors has made the internally isolated detection of tagged materials very possible.

Measurements of gaseous mutual diffusion and self-diffusion coefficients have usually been made at moderate pressures where the mean free path length is much smaller than the dimensions of the vessel in which the measurements were made. Only in recent years have attempts been made to measure these diffusion coefficients at low pressures when the gas movement is confined to

tiny channels in porous beds or capillary tubes. The apparatus used in this study was designed to measure diffusion through a capillary tube in the transition pressure range by utilizing a radioactive tracer. While radioactive tracers have been used by several experimenters to measure diffusion coefficients, the use of a semiconductor detector as the radiation sensing device in conjunction with such experiments is believed to be novel. The advantages of this method are illustrated by a review of earlier techniques.

2.2 Methods of Measuring Diffusion Coefficients

The classical method for determining diffusivity in gaseous systems is to measure the time required to produce a concentration change when two different gases are allowed to diffuse into each other after an initial separation. Early measurements based on this classical approach utilized the method of Loschmidt (18,57). Loschmidt used a glass tube 97.5 cm in length and 2.6 cm in diameter supported vertically and divided at the center into two parts by a partition. The top half of the tube was filled with the light gas and the bottom half with the heavy gas, both at the same temperature and pressure. The mutual coefficient was found by comparing the observed average concentration changes in both tube sections to a solution of the second order partial differential equation describing the diffusion process in the Loschmidt apparatus. If the same apparatus is used and the pure gases are replaced by gas mixtures of slightly different concentrations the slight variation of D with concentration can be neglected and one obtains a diffusion coefficient based upon the mean composition of the initial mixtures. The concentration of gases in the diffusion tube can be measured by several methods of gas analysis such as gravimetric analysis after reacting and/or absorbing the gases in a solid,

by thermal conductivity methods or by a spectrometer. Tordai (82) has presented a comprehensive study of the errors in diffusion measurements by the Loschmidt method indicating potential accuracies to within 0.3%. Strehlow (77) used a modified Loschmidt cell to study the temperature dependence of the mutual diffusion coefficient for four gaseous systems. He reported D values with less than 2% error.

In 1951, Boyd, Stein, Steingrimsson, and Rumpel (10) described a new type of experimental method for accurately measuring gaseous mutual diffusion coefficients which was based upon the Loschmidt geometry. To trace the change in composition, they measured the refractive index of the gas at a fixed position in their rectangular diffusion cell (12.6 cm x 2.2 cm x 38.1 cm) with an interferometer. Their method allowed several determinations of D, accurate to within 0.5%, during one experimental run. The diffusion data was taken from photographs of interference fringes occuring at specified times.

In 1962 Giddings and Seager (34) suggested a method similar in operation to chromatographic techniques for making rapid determinations of binary gaseous diffusion coefficients. The apparatus used consisted of a gas chromatography unit, with an empty tube replacing the packed column. They reported binary coefficients for eleven different gas mixtures which agreed to ± 1% with other values reported in the literature. While this apparatus is being modified to improve the accuracy of the coefficient measurements and to broaden the applicability to other diffusion problems, it is unlikely that this technique can be utilized to determine gas diffusion coefficients in the transition pressure range.

The method of Stefan (55) has been used in recent years to measure

diffusion coefficients in gaseous systems (15). By this method the diffusivity of a gas pair is determined by observing the steady-state evaporation of the liquified gas into a tube containing the other gas. The distance between the liquid level and the top of the tube, the total pressure on the system, the vapor pressure of the liquid, and the temperature of the system must be determined to allow calculation of the diffusion coefficient. The volume of liquid evaporating during a certain time period reflects the diffusivity of the gas pair. Several defects can be attributed to this method of determining gas-phase diffusivities. Convection effects may occur if the vapor of the evaporating liquid is lighter than the gas in the column. Also due to the liquid phase miniscus the length of the diffusion path will vary across the tube diameter. The cooling effect of the liquid evaporation is probably the most significant defect of this method.

Using a Loschmidt cell Boardman and Wild (8) were the first to simulate the conditions for self-diffusion by using gases with molecules of equal mass. Using mixtures of nitrous oxide and carbon dioxide, D_{11} for either gas was found to be 0.0107 cm^2/sec at 288°K and 76 cm pressure. They also reported values of D_{11} for hydrogen, nitrogen and carbon dioxide calculated by the method of Kelvin triads using their diffusion data for H_2-N_2, N_2-CO_2, and CO_2-H_2 systems. In the method of Kelvin triads, the coefficient of mutual diffusion is determined for each of the three pairs which can be chosen from three gases. The corresponding σ_{12} can be determined from equations based on the rigid elastic sphere model. Since $\sigma_{12} = 1/2(\sigma_{11} + \sigma_{22})$ the values of σ_{11} for each of the three gases in the triad can be found. Substitution of σ_{11} into the appropriate formula (see Eq. 5) gives D_{11}.

Knudsen (53), Gaede (33), and Adzumi (1) were the first investigators

to study the flow of gases through long capillary tubes. In the Knudsen apparatus, the capillary tube was connected between two chambers having volumes of approximately 1000 cc each. The flow of gas from one chamber to another was interrupted by means of a mercury cut off valve. Knudsen demonstrated that a minimum specific flow occurred when r/ℓ was approximately equal to 0.3. Gaede, using similar apparatus with a rectangular slit in place of the capillary tube, verified Knudsen's findings of the existence of a minimum specific flow, but erroneously attributed the minimum to the formulation of an adsorbed layer on the channel wall restricting flow. The investigation of Adzumi which verified Knudsen's results also duplicated that of Knudsen but was accomplished for several tube diameters at both low and intermediate pressures.

The closest approximation to real self-diffusion is accomplished by the use of isotopic molecules. The intermolecular forces and molecular cross sections for the interaction between isotopic molecules are essentially the same as for the interaction between identical molecules of the isotopic pair. Harteck and Schmidt (38) were the first to use this method to find D_{11} for a gas. They used the Loschmidt method with para-hydrogen diffusing into normal hydrogen. The concentration change was determined by thermal conductivity measurements. Applying the same technique, Groth and Harteck (36) determined D_{12} for krypton and xenon mixtures using isotopes.

In 1943 Ney and Armistead (59) developed a more accurate method for making isotopic-diffusion measurements. Their apparatus was similar in design to that of Knudsen, but incorporated the use of a mass spectrometer for concentration measurements. Since the Ney-Armistead technique has been used for nearly all subsequent measurements of self-diffusion, including the

present one, it is described in considerable detail below.

The Ney-Armistead apparatus was similar to that of Knudsen in that two large chambers were used with a straight tube connecting them. In the original apparatus two copper tubes with a short section of neoprene tubing between them connected the two diffusion bulbs having volumes of 925 and 259 cc. One chamber was charged with $U^{235}F_6$ and the other with $U^{238}F_6$, both at the same temperature and pressure. When the clamp on the rubber tube was released the diffusion process started and samples from one chamber were bled through an adjustable capillary leak to a mass spectrometer. The decrease of gas pressure in the open chamber did not cause diffusion measurements to be in error by more than 1%. The reported cumulative error in measurements of the geometrical constants was about 3% while the error in pressure measurements (approximately 1000 microns) was less than 1%. Diffusion coefficients were reported to within 4%. This method had two definite advantages over the Loschmidt technique: (I) greater compactness, thus reducing the errors associated with temperature gradients and (II) the facility for making continuous concentration measurements and, thereby, several diffusion coefficients during one run.

The theory for the Ney-Armistead technique is based on certain simplifying assumptions. The diffusion equation used assumes the diffusion coefficient to be independent of concentration which is justified for the case of self-diffusion, but not for mutual diffusion. According to kinetic theory the mutual diffusion coefficient is independent of concentration only in the first approximation. The experimental theory for this method is based upon three additional assumptions; namely (i) the concentration gradient in the connecting tube varies linearly with distance along the tube, i.e., $\partial c/\partial z = \text{const.}$,

(ii) perfect continuous mixing exists in the flasks, the concentration gradient being confined to the connecting tube, (iii) the volume of the connecting tube is negligible compared with the chamber volume. A discussion on the validity of these assumptions including the corrections necessary have been presented by Paul (64). The small correction necessary for assumption (i) is proportional to the ratio of the volume of the capillary tube to the volume of the chambers. The second assumption that the gradient exists only in the connecting tube is justified provided a small end correction is made. The magnitude of the correction for the analogous electrical case has been shown by Maxwell (58) and Rayleigh (78) to be an increase in L, the tube length, by 0.82 times the radius. A correction for assumption (iii) is made by adjusting the concentration in both chambers to account for the effect of the tube volume. Using the above assumptions, Fick's second law (19) is used to write an equation describing the transport of the trace gas through the capillary tube. The resulting second order partial differential equation is solved for the appropriate boundary conditions and utilized in determining the diffusion coefficient from the concentration data.

Nearly all recent measurements have utilized isotopes and the Ney-Armistead apparatus. Winn and Ney (90) investigated methane self-diffusion while the $N^{14}N^{14}$-$N^{14}N^{15}$ system was investigated by Winn (88), both using the Ney-Armistead apparatus.

Hutchinson(47) has shown that the self-diffusion coefficient of a gas can be obtained from the coefficient of diffusion of one isotope into another by the following relation:

$$D_{11} = \left[2m_2/(m_1+m_2)\right]^{1/2} D_{12}. \qquad (24)$$

He determined the coefficient for argon (46) at five different temperatures

between -183°C and 53.5°C by observing the diffusion of A^{41} into argon with a modified Ney-Armistead apparatus. Two metal chambers, each of about 100 cc volume, were connected by a straight tube 0.475 cm diameter and 2.85 cm long drilled through a steel block containing a sliding valve used to close off the connecting tube. The concentrations of A^{41} in both chambers were determined by the ion currents drawn to insulated electrodes inserted into each chamber. Using non-radioactive isotopes for A, Ne, N_2, O_2, CO_2 and CH_4, Winn (89) also studied the temperature dependence of self-diffusion coefficients. His apparatus avoided the use of a cutoff valve in the capillary tube by filling both chambers simultaneously to the same pressure with different concentrations of isotopes.

The radioactive tracer, $C^{14}O_2$ has been used frequently to measure diffusion coefficients. Recently, Winter (91), Visner (83), Amdur and coworkers (3), Timmerhaus and Drickamer (81), Jeffries and Drickamer (48), O'Hern and Martin (60) and Amdur and Schatzki (2) have used $C^{14}O_2$ or A^{41} as a trace gas in modified Loschmidt and Ney-Armistead cells. Amdur measured diffusion coefficients within 2% for CO_2-CO_2, CO_2-N_2O, Xe-Xe, and A-Xe systems using a Loschmidt device. The ionization currents from two collecting electrodes, one in each section of the diffusion chamber, were used to measure concentration changes. The work of Drickamer utilized a scintillation detector in a modified Loschmidt cell to measure diffusion coefficients of CO_2-CO_2 and CO_2-CH_4 systems over a pressure range from 0.5 to many atmospheres. The diffusion tube was filled with several types of packing to accommodate the higher pressures; therefore, it was necessary to overlap the runs to determine the effective path length for each type of packing. Diffusion coefficients for carbon dioxide were determined by O'Hern and Martin from 0°

to 100°C and at pressures to 200 atm. The data reported demonstrated that the diffusion coefficient is approximately proportional to the reciprocal of the density within the ranges of conditions considered. The diffusion cell used was similar to that of Hutchinson, using ionization chambers to determine concentration changes. It differed in that a porous metal plug was inserted in the diffusion chamber and no means existed for closing the diffusion opening when the two chambers were filled with gases. The entire system was filled with carbon dioxide before the radioactive gas was added to one chamber. Winter used a Ney-Armistead apparatus to measure diffusion coefficients of CO_2, O_2 and N_2. The diffusion cell contained a large bore stopcock at one end of the capillary tube connecting the flasks. After filling both flasks with the heavy gas the capillary valve was closed and the gas in one flask withdrawn and replaced with an equal amount of the normal gas. The accuracy of the measurements reported was within ± 1%. Visner (83) has made the only study of gas diffusion in the transition pressure range using a diffusion tube with well defined dimensions, i.e., an empty capillary tube instead of a chamber packed with porous material. He used a modified Ney-Armistead cell with end-window Geiger counters installed in both flasks to follow concentration changes. The self-diffusion coefficient of xenon was measured for capillaries of 0.0025 cm and 0.025 cm radius in tubes of three lengths for pressures corresponding to radius to mean free path ratios from 0.001 to 65. The trace gas was injected into one flask after filling the flasks to the desired pressure with normal gas by breaking a tiny glass bulb of gas at the correct pressure to prevent the creation of a pressure gradient across the capillary tube.

An apparatus called a diffusion bridge was used by Bendt (4) to measure

the diffusion coefficient for He^3-He^4 and H_2-D_2 at one atmosphere pressure and temperatures from 1.74°K to 296°K. The measurement was made while steady-state flow existed through four capillaries and through the diffusion tube which joined the supply and exhaust capillaries in the temperature bath. The pressure gradient in the diffusion tube was made as small as possible by adjusting the flow rates of the gases through the capillary feed lines. The exhaust capillaries were alternately connected to a mass spectrometer for gas analysis. Small fluctuations in the flow rates and in the sensitivity of the mass spectrometer limited the accuracy of the measurements to an error of 2-6 %. The correction factors used were the Rayleigh tube length correction and the mass correction formula (Eq. 24) for isotopic self-diffusion measurements.

Recently, a new method (69,86) has been designed for making diffusion measurements of gases at elevated temperatures. In this method a point source of trace gas is injected into a slow uniform stream flowing through a conduit. The variations in the concentration as a function of radius and time are measured to determine the diffusion coefficient. The primary use of this method has been to study gaseous diffusion at high temperatures and pressures.

The above survey has included a discussion of all common techniques used to measure diffusion coefficients. The Ney-Armistead method has been emphasized because it allows a simple and accurate means of studying gas diffusion in the transition pressure range. Additional surveys of recent experimental and theoretical work on the diffusion of gases have been made by Liley (56) and Johnson (49,50,51). A discussion of information on diffusivity needed by the chemical and process industries has been presented

by Friend and Adler (32).

2.3 Analysis

The transient-type diffusion apparatus used in this study was similar to the Ney-Armistead apparatus described above. Figure 2 is a schematic representation of the one-dimensional diffusion system employed. Flasks I and II were filled with gas at the same pressure and temperature, while the gas in flask I contained a trace quantity of radioactive gas. When the capillary valve "10" was opened a process of one dimensional diffusion was established in which molecules of flask I intermixed with molecules of flask II, finally resulting in a system of constant composition. The amount of self-diffusion occurring was determined by observing the change in radioactivity in flask I as a function of time with a semiconductor radiation detector.

All of the assumptions presented above for the Ney-Armistead apparatus were applicable to the apparatus pictured in Fig. 2 except that the tube volume was not considered to be negligible. Based upon these assumptions it was possible to represent the one dimensional diffusion process by utilizing Fick's second law (19). The resulting partial differential equation for diffusion through the capillary tube was

$$\frac{\partial C}{\partial t} = D \frac{\partial^2 C}{\partial z^2} \tag{25}$$

with C = the concentration of trace gas at time t, D = the diffusion coefficient, and z = the coordinate along which the diffusion was occurring.

Equation (25) was solved for the boundary conditions:

$$t = 0,\ z>0,\ C = 0 \tag{26}$$

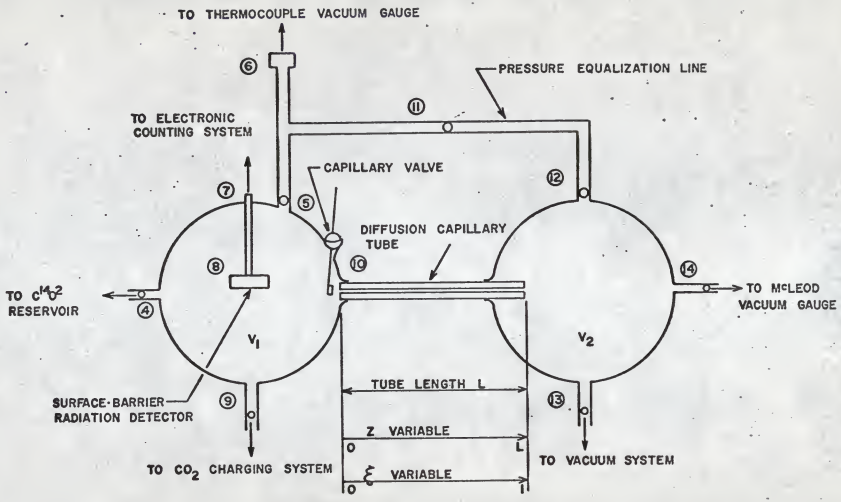

Fig. 2. Simplified experimental diffusion cell assembly with system parameters.

$$t>0,\ z = 0,\ C\Big|_{z=0} = C_o - 1/V_1 \int_0^t -D(\pi R^2)\left.\frac{dC}{dz}\right|_{z=0} dt \qquad (27)$$

$$t>0,\ z = L,\ C\Big|_{z=L} = C_o V_1/V_2 - CV_1/V_2\Big|_{z=0} - 1/V_2 \int_0^L C(\pi R^2)dz \qquad (28)$$

where V_1 = volume of the tagged reservoir

V_2 = volume of untagged reservoir

L = effective tube length

R = radius of tube

C_o = concentration of tagged material at zero time in the tagged reservoir.

C = concentration of tagged material as a function of t and z.

These boundary conditions mathematically represent the physical requirements of the system. Equation (26) indicates that at zero time the capillary tube contains none of the tagged isotope. Equation (27) shows that the composition of the tagged isotope in flask I is the original amount less the total amount leaving flask I by diffusion into the capillary tube. Boundary condition Eq. (28) states that the composition of trace gas in flask II, under conditions of uniform mixing, represents the amount of material diffusing into the tube from flask I less the amount still remaining in the capillary tube.

The complete solution to Eq. (25) is

$$X(\tau,\xi) = \beta\left[\alpha + \beta + \alpha\beta\right]^{-1} - \sum_{n=1}^{\infty}\left[\exp(-\lambda_n^2\tau)\right]\left[\lambda_n \cos\lambda_n + \beta \sin\lambda_n\right] \cdot \left[\alpha\cos(\lambda_n\xi) - \lambda_n \sin(\lambda_n\xi)\right]\left\{\lambda_n^2\left[(2\lambda_n)^{-1}(\cos\lambda_n)(\alpha + \beta + \alpha\beta - \lambda_n^2) - \sin\lambda_n(1 + 1/2(\alpha + \beta))\right]\right\}^{-1} \qquad (29)$$

where λ_n are the non zero roots of

$$\tan \lambda_n = \lambda_n(\alpha + \beta)\left[\lambda_n^2 - \alpha\beta\right]^{-1}. \qquad (30)$$

A detailed solution of Eq. (25) by the method of Laplace transforms is given in Appendix A.

The time response of this system can be seen from Fig. 3 where the concentration in the CO_2-N_2 system at 25°C is shown as a function of pressure for both the bulk and Knudsen range coefficients. The Knudsen line corresponds to a pressure of 89.2 microns of mercury where the diffusion coefficients are identical. It can be noted that for this size tube the diffusion is retarded enough so that extremely accurate short time measurements are not required. The response of the system is easily changed by varying the tube length.

Equation (29) relates the concentration of the tagged gas to time at a position z inside the cell in terms of the diffusion coefficient, D, and the cell dimensions. An application of least squares analysis (61) to the concentration versus time data using Eq. (29) and the appropriate system parameters yields an evaluation of the diffusion coefficient. A detailed discussion of the procedure for applying least squares analysis to the evaluation of D is given in Appendix C. In this experiment the tube length was determined by measuring and applying the Rayleigh end-correction used by Ney and Armistead. The other system parameters were measured as outlined in section 2.6.

Based upon the assumption of continuous mixing at the pressure of the measurement, which has been shown to be valid by Visner (83), the radioactivity measured by the surface-barrier detector was linearly proportional

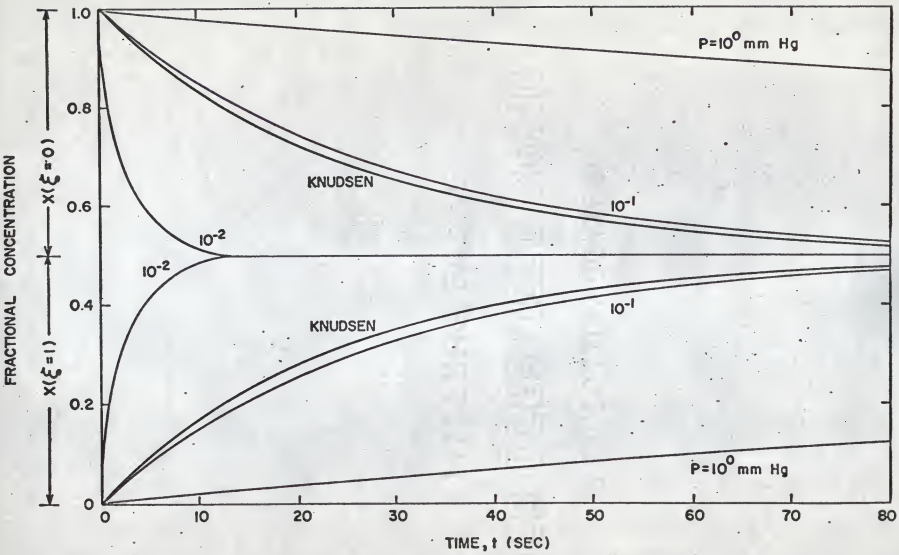

Fig. 3. Transient response curves for a 0.05 cm radius and 10 cm length capillary tube showing Knudsen pressure crossover for $C^{14}O_2$ in CO_2-N_2 system.

to the concetration of CO_2 in flask I. Due to the rapid response, the thin window, and the high counting efficiency of the detector it was not necessary to make dead time or other corrections on the activity data. The properties of semiconductor detectors are discussed in section 2.4.

2.4 Semiconductor Radiation Detectors

During the last five years rapid development of solid-state semiconductor detectors (11,20,23,43,44,67) has gained for this type of detector prominence in the field of nuclear radiation detection. Semiconductor detectors have several characteristics which give them advantages over gas and scintillation counters for many applications. The chief advantage is that these detectors approximate an ideal ionization chamber wherein the usual gas has been replaced with a semiconducting solid having high stopping power. The number of free charge carriers produced by the absorption of an amount of energy (approximately one free electron-hole pair per 3.5 ev. of particle energy) is independent of the mass and the total energy of the incident radiation; therefore, the electric signal response is linearly proportional to the energy deposited by a particle in the sensitive region (depletion region) of a detector. These detectors can be constructed to have the additional advantages of small size, low weight, rigidly controlled sensitive depth and geometry, thin window thickness, long term stability and durability, low operating voltage, and rapid time response.

The junction between an n-type, or donor-rich, region and a p-type, or acceptor rich, region is utilized in forming semiconductor detectors (75,80). A reverse bias applied to the interface between an n-type and p-type material causes the development of a charge-deficient, highly resistive region called

the depletion region. This depletion region is formed by movement of electrons from the n-type material toward the p-type material and holes from the p-type material toward the n-type material. The separation of holes and electrons causes a space-charge region due to an unbalanced concentration of filled electron acceptor sites and positively charged empty donor sites on opposite sides of the junction. The space-charge region is the sensitive volume of the detector in which electron-hole pairs produced by ionizing radiation are collected; thus, causing the origination of the output signal. The depth of the sensitive volume is proportional to the square root of the product of applied bias voltage and dielectric resistivity. The depletion depths range from 2000-3000 microns and depend upon the type of detector used.

The three types of semiconductor detectors are (i) silicon-diffused junction detectors, (ii) lithium-drifted silicon or germanium detectors, and (ii) silicon surface-barrier detectors. A diffused junction detector is made by diffusing n-type phosphorus into p-type (boron doped) silicon while the surface-barrier detector is made by evaporating a thin p-type layer of gold on the surface of n-type silicon. The thickest depletion layers occur in the lithium-drifted detectors which are formed by forcing n-type lithium ions deep into p-type silicon or germanium. Each detector type has characteristics which give it distinct advantages for certain applications (6,7). In the experimental work of this study, a silicon surface-barrier detector was the radiation sensing device employed. An excellent discussion of the properties and applications of the three types of semiconductor detectors is given by F. S. Goulding (35).

The surface-barrier detector will count any charged particle which is

incident upon the sensitive gold surface if it arrives with sufficient energy and at the proper angle to penetrate the gold surface and at least a small portion of the depletion region in the silicon. When the charge carriers created by an incident radiation are separated by the electric field they attain a drift velocity in the silicon toward the electric poles. The motion of the carriers induces a charge in the external circuitry. Use of a pre-amplifier with a charge sensitive input circuit having negative capacitive feedback results in a voltage pulse which is approximately independent of detector capacitance.

Noise sources are present in the detector and the amplifier and the accuracy of measuring the size of the signal is directly related to the ratio of real signal to noise. Microplasma breakdown, edge leakage currents, and charge carrier generation and recombination in the depleted region are the primary contributors to detector noise. These factors are minimized by selecting a quality detector that has a thin, small volume depletion region and by operating at minimum temperature. On the other hand, the detector electrical capacity must have a low value to give a good signal-to-noise ratio. The detector capacity varies directly with the detector area and inversely with detector thickness. Obviously, a compromise must be made in selecting the depletion layer thickness and it depends largely upon the intended use of the detector. A discussion of the fundamentals of low-noise preamplifiers is given by Fairstein (31), while a guideline for preamplifier selection is given by Radeka (68).

Since the surface-barrier detector is a highly sensitive instrument, several rigid requirements are necessary to insure proper operation. All signal leads and the detector must be shielded to prevent electronic pickup.

The cable between the detector and preamplifier should be as short as possible to minimize input capacitance. The bias voltage must come from a well-filtered, stable, and well-regulated supply. All electronic equipment must be tied to a common ground to avoid ground loop problems. The detector is photosensitive and must, therefore, be installed in a light tight enclosure.

To guarantee full detector operating capability it is necessary to monitor the noise level when applying the bias. After an initial increase, the noise level of the detector increases with bias voltage until a breakdown voltage is reached. However, a sufficiently high electric field is required to insure fast and efficient charge collection, so that an optimum bias setting value must be chosen. The noise level can be measured with a RMS voltmeter, an oscilloscope, or a multichannel analyzer.

To prevent damage, several precautions must be observed when using the surface-barrier detector. The sensitive gold surface must not be touched when handling the detector. A mechanical stress, such as is caused by changing the ambient pressure on the detector, and an electrical stress, such as changing the detector bias, should not be applied simultaneously. Any stress applied should be gradual. Care must be taken to avoid chemical contamination from mercury and oil vapors or other contaminants. The detector is damaged by continued exposure to high radiation fluxes, and should, therefore, be shielded from unnecessary radiation. And finally, one should always prevent the application of excessive bias voltage which produces irreversible damage to the semiconductor material.

2.5.0 Experimental Facilities

A diffusion cell apparatus and an electronic counting system comprised the experimental facilities used in making all measurements. With a radioactive component diffusing from one flask to a second flask joined by a capillary tube, the radioactivity in the charged flask provided a continuous measurement of the diffusion occurring through the opening in the capillary tube. The diffusion cell employed had similarities to those of earlier investigators, especially to those of Hutchinson (46), O'Hern and Martin (60), Winter (91), Ney and Armistead (59), and Timmerhaus and Drickamer (81). Figures 4, 5, and 6 illustrate the diffusion cell and auxiliary apparatus. The electronic counting system, diagrammed in Fig. 7 and pictured in Fig. 8, consisted of a semiconductor radiation detector and a scaling circuit.

2.5.1 Diffusion Cell and Auxiliary Apparatus

A top view of the Pyrex glass diffusion cell mounted in the unfilled water bath is shown in Fig. 5. Referring to either Fig. 4 or Fig. 5, flask I represents the side of the system charged with radioactive carbon dioxide and containing the surface-barrier semiconductor radiation detector. The detector was installed in flask I, suspended from two No. 22 tungsten wire leads passing through a removable S 34/45 ground glass cover. The capillary tube and a pressure equalization tube "11" provided vacuum tight connections between flask I and flask II. The length and the internal diameter of the precision bore capillary tube were found to be 10.120 cm and 0.1027 cm respectively. The diameter was determined by measuring the length and mass of a thread of mercury inside the tube (22). High vacuum stopcocks were

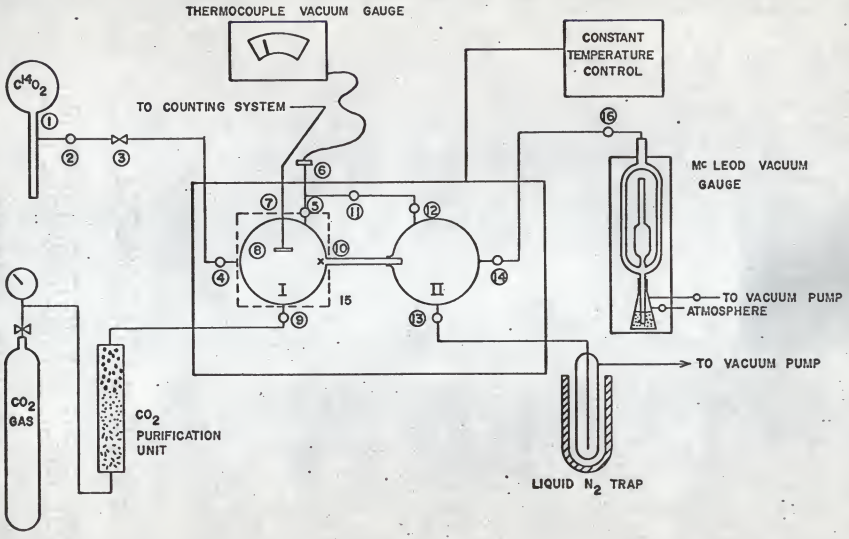

Fig. 4. Schematic diagram of diffusion cell and auxiliary apparatus.

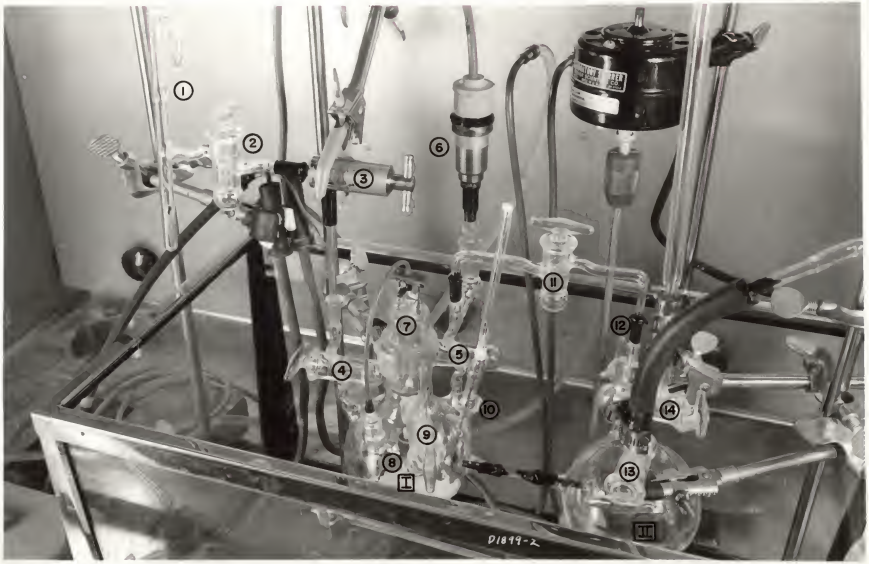

Fig. 5. Assembly of diffusion cell apparatus (electrical and light shields not shown).

Fig. 6 Surface-barrier radiation detector before insertion into operating position.

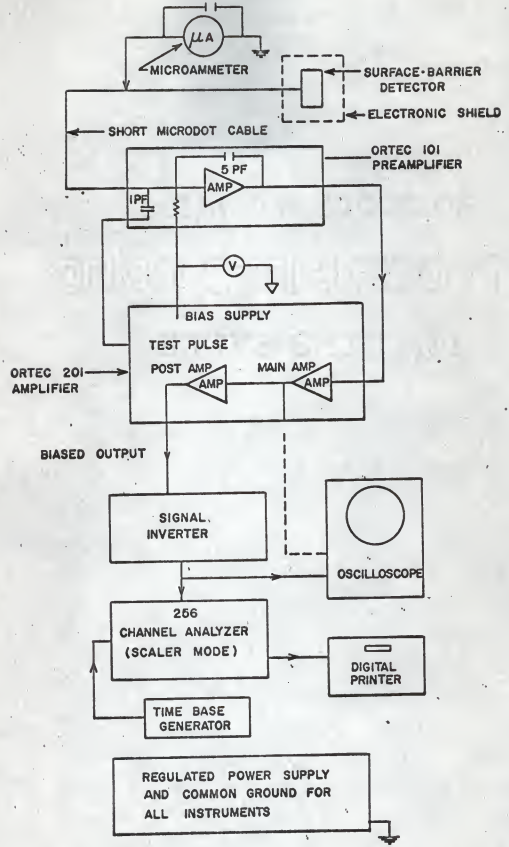

Fig. 7. Block diagram of complete counting system.

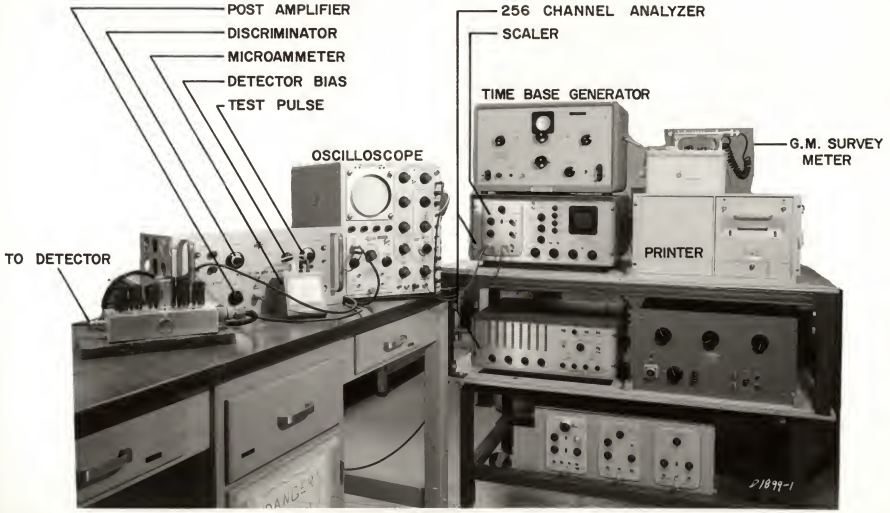

Fig. 8. Assembled electronic counting system.

used to control gas flow through the six orifices in flask I and II, through the pressure equalization tube, and to the thermocouple vacuum gauge tube "6" (See Appendix B for detailed experimental procedure). Flasks I and II had volumes of 545 ml and 512 ml, respectively. The capacities of these flasks, up to the bottom of the ground glass joint (see Fig. 4), were determined by filling with a measured quantity of water.

A stiff molybdenum wire passing through a spherical ground glass joint provided a lever arm for operation of the capillary tube valve "10". A small piece of polyethylene was fastened to the end of the wire so that it covered the end of the capillary tube when the valve was in the closed position. Although this valve did not provide a vacuum-tight seal on the capillary tube, it did reduce the flow through the tube to negligible quantities during short waiting periods when the valve was closed. This capillary tube valve, which differed from those of many earlier diffusion set-ups, was designed to prevent any discontinuities or irregularities along the diffusion path.

Radioactive and nonradioactive carbon dioxide flowed to flask I through stopcocks "4" and "9" respectively. The nonradioactive gas (greater than 99% pure) was purified in a tube of Drierite, silica gel, and magnesium perchlorate. A glass ampoule supplied by Volk Radiochemical Company containing 0.10 mc of $C^{14}O_2$, having specific activity 1mc/mM (0.01 % vol $C^{14}O_2$), provided the trace gas for all measurements made. After the diffusion cell was purged three times with natural carbon dioxide and the desired equilibrium pressure obtained, trace gas was throttled into flask I through the Hoke capillary valve "3".

A Kenney thermocouple vacuum gauge (Model KTG-1) was utilized in measur-

ing the carbon dioxide pressure in the diffusion cell. The installation of gauge tube "6" in series with stopcock "5" and stopcock "11" allowed measurement of the equilibrium pressure when stopcock "11" was open and of the pressure in flask I when stopcock "11" was closed.

An upright McLeod vacuum gauge (range 0.05 to 500 microns) connected to flask II, "14", was used in calibrating the thermocouple gauge. A linear relationship was found to exist for the calibration between the gauge reading and absolute pressure in the range of interest (0 - 500 microns). The vacuum gauge meter could be read approximately to ± 1% between 5 and 10 microns, to ± 5% between 70 and 200 microns, to ± 7% between 200 and 300 microns, and to ± 10% at higher pressures. The absolute accuracy and reproducibility of the gauge was stated by the manufacturer to be ± 10% at 50 microns.

A 12 gallon tank filled with water served as a constant temperature ($20^{\circ}C$) bath for the diffusion cell (95% immersed). Constant temperature regulation to ± $0.5^{\circ}C$ was provided by a thermoregulator and relay which controlled a low wattage heating element. Tap water ($16.5^{\circ}C$) running through a coiled copper tubing served as the heat sink.

The diffusion cell, together with all auxiliary equipment containing radioactive gas, was housed in a high velocity hood to guard against exposure to radiation. A liquid nitrogen trap installed between stopcock "13" and the two-stage, oil sealed mechanical vacuum pump prevented the escape of radioactive gas through the pump exhaust. The cold trap was periodically removed to allow accumulated $C^{14}O_2$-CO_2 solid to sublime and be expelled slowly through the hood exhaust.

2.5.2 Electronic Counting System

The ability of an electronic counting system to detect low energy beta particles, such as those emitted by carbon-14 (E_{max} = 156 kev (54)) has been shown to be dependent upon the signal to noise ratio of the amplified detector output. If noise amplitude is high compared to signal amplitude, it is usually not possible to separate the spurious counts from those that are real. If, on the other hand, the signal-to-noise ratio is large it is possible to electronically discriminate against the noise pulses and count only the pulses produced by radiation incident upon the detector. For the case of polyenergetic C^{14} beta particle detection, part of the real signal is always discriminated out with the noise. Thus, the detection system used in this experiment was designed to develop a minimum amount of noise. It is most important that the production of noise is prevented at that point in the counting system where the real signal is the smallest, i.e., at the detector where the signal is created.

Because the surface-barrier radiation detector was extremely sensitive to electromagnetic radiation, it was necessary to construct an electrical and a light shield surrounding the glass flask housing the detector. A fine-mesh brass screen jacket built around flask I (see Fig. 6) and grounded to the preamplifier chassis was effective in shielding against stray electrical signals. The complete outer surface of flask I, except for small parts of stopcocks "4", "5", and "9", was painted with black Glyptal paint. Since the capillary tube served as a light pipe between the two flasks, part of flask II was also painted. Detector surface leakage was avoided by handling the detector with extreme care. Thermal noise in the detector was minimized by maintaining the detector as a constant temperature.

A five inch long microdot shielded cable connected the detector leads to an ORTEC low noise preamplifier (Model 101). This cable was made as short as possible to reduce input capacitance since the signal voltage was inversely proportional to the sum of the effective detector capacitance and all other input capacitances. The preamplifier utilized a charge-sensitive input circuit and a voltage amplifier provided with a negative feedback path allowing it to simulate a charge-to-voltage transducer. Signals emerging from the preamplifier had an amplitude of several millivolts.

The preamplifier was connected to the ORTEC low noise amplifier (Model 201) through a shielded cable. This amplifier chassis contained the power supplies, the 60 cycle test pulse generator, the discriminator bias circuit, and the main and post amplifiers. A microammeter measuring detector current leakage and a Tektronix oscilloscope (Type 545) with visual display of the amplified signal were used simultaneously to monitor the noise level as the detector bias was increased. The proper discriminator setting was selected by observing the scope display in the absence of a radioactive source. The positive signal output of the post amplifier was inverted and attenuated by a Tektronix power supply (Type 132) with CA plug in unit to make it compatible with the 256 TMC multichannel analyzer (scaler mode).

A square wave from a Hewlett-Packard low frequency generator was used as the external time base for the analyzer. The wave frequency was variable between 0.001 and 150 cycles per second. The paper tape containing the experimental data was printed with a Hewlett-Packard digital recorder (Model 561-B). Serious ground loop and line transient problems were alleviated by connecting all electronic equipment, excluding the scope, to a well regulated Beckman power supply.

2.6.0 Reduction of Data

2.6.1 Preparation of Data for Analysis

Several operations on the data were required before the computer program could be applied to solve for the diffusion coefficient. It was, of course, necessary to associate a time with the activity represented by each channel of the multichannel analyzer. The dimensionless variables used in the solution to the one dimensional diffusion equation required that the counts per channel, which represented the concentration of $C^{14}O_2$ in flask I, be normalized to the count rate at time zero when no diffusion had occurred. The technique for eliminating a pressure gradient in the diffusion cell (see Appendix B) allowed some radioactive gas to flow into flask II and thereby increased the equilibrium count rate to a value larger than that predicted by the mathematical model. Thus, without violating any of the assumptions made in the analysis, a background count rate was subtracted from the data. The procedure for performing these operations is outlined in the following paragraphs.

Before designating a time to each of the 256 counting rates produced by the 256 channel analyzer, the data points were divided into groups of ten and added. This procedure decreased the number of data points without altering the profile of the diffusion process which had occurred and substantially decreased the computer time required for the analysis. When some of the channels in a group were missing because the analyzer "dropped" counts, the counts present were added and their magnitude adjusted to represent ten channels. The time associated with each group of counts was determined by using the constant time increment per channel controlled by the time base

generator. Each group was given the time associated with its middle channel. A sample set of analyzer output and the corresponding reduced data are given in Tables I and II.

The unequal volumes of flasks I and II caused the normalized equilibrium concentration, C_∞/C_o, to equal 0.51562 if flask II contained no radioactive gas at time zero. Since in the actual experiment some $C^{14}O_2$ did escape to flask II before the zero-time concentration in flask I was measured, the experimental normalized equilibrium concentration was larger than 0.51562, e.g., 0.5950 in the sample data set. In adjusting the data to fit the model a constant, x, was subtracted from each number of counts. The constant was determined by using the following relationship

$$(Cts(\infty) - x)/(Cts(0) - x) = 0.51562 \qquad (31)$$

where the equilibrium number of counts, Cts(∞), was taken as the average of the last several data points at which the diffusion process had reached equilibrium. After subtracting the "background" count from each datum point, the data were normalized by dividing each by the corrected number of counts at zero time. A sample set of normalized concentration versus time data is given in Table III. It is noted that the data in Table I, II, and III correspond to a common experimental run at a pressure of 210 microns. An application of least squares analysis to the sample data yielded 319.4 cm^2/sec for the diffusion coefficient.

2.6.2 Error Associated with the Determination of D by Least Squares Analysis

Errors incurred in the experimental measurements of count rate caused considerable scatter of the data about the mathematical curve representing

Table I. Sample multichannel analyzer output

Channel	Counts	Channel	Counts
1	0000	47	1576
2	2057	48	1614
3	2062	49	1526
4	2110	50	1611
5	0013	51	1580
6	2051	52	1526
7	2021	53	1600
8	2017	54	1543
9	1185	55	1522
10	1672	56	1576
11	1974	57	1558
12	1848	58	1533
13	1538	59	1485
14	1800	60	1548
15	1932	61	1503
16	1910	62	1493
17	1855	63	1595
18	1842	64	1492
19	1868	65	0399
20	1851	66	0160
21	1832	67	1508
22	1833	68	1544
23	1720	69	1436
24	1729	70	0442
25	1756	71	1476
26	0694	72	1506
27	1802	73	0008
28	1743	74	1448
29	1720	75	1484
30	1815	76	1483
31	1707	77	0384
32	1712	78	0426
33	1701	79	1398
34	1730	80	1426
35	1697	81	1407
36	1713	82	1417
37	1633	83	1411
38	1707	84	1424
39	1729	85	1436
40	1593	86	1392
41	1625	87	1354
42	1703	88	1409
43	1611	89	1355
44	1595	90	1384
45	1646	91	1351
46	1588	92	1379

Table I (continued)

Channel	Counts	Channel	Counts
93	1390	139	1296
94	1351	140	1307
95	1363	141	0007
96	1395	142	1298
97	1360	143	1312
98	1328	144	1328
99	1432	145	1310
100	1404	146	0212
101	1340	147	1272
102	1373	148	1289
103	1375	149	0201
104	1414	150	1298
105	1326	151	1258
106	1381	152	1264
107	1367	153	1315
108	1338	154	0226
109	1366	155	1326
110	1327	156	1282
111	1374	157	1284
112	1355	158	1292
113	1345	159	1253
114	1339	160	1288
115	1305	161	1255
116	1313	162	1302
117	1335	163	1257
118	1322	164	1267
119	1404	165	1207
120	1305	166	1239
121	1343	167	1280
122	1307	168	1352
123	1295	169	1208
124	1350	170	0130
125	1311	171	1299
126	1327	172	1300
127	1294	173	0223
128	1229	174	1309
129	1252	175	1266
130	0018	176	1287
131	1284	177	1300
132	1329	178	1260
133	1284	179	1251
134	1333	180	1207
135	1345	181	1183
136	1317	182	1307
137	1296	183	1282
138	0000	184	1247

Table I (continued)

Channel	Counts	Channel	Counts
185	1280	229	1116
186	1298	230	0143
187	1273	231	1184
188	1198	232	1240
189	1257	233	0187
190	1256	234	1153
191	1262	235	1202
192	1272	236	1270
193	0000	237	1205
194	0000	238	1287
195	1248	239	1240
196	1217	240	1275
197	0000	241	1182
198	0008	242	1226
199	1230	243	1244
200	1250	244	1226
201	0132	245	1219
202	0032	246	1276
203	1262	247	1229
204	1239	248	1240
205	0000	249	1242
206	0012	250	1238
207	1302	251	1194
208	1292	252	1296
209	1265	253	1186
210	1281	254	1201
211	1240	255	1281
212	1230	256	1254
213	1257		
214	1281		
215	1292		
216	1238		
217	0022		
218	0180		
219	1256		
220	1251		
221	0278		
222	0154		
223	1267		
224	1195		
225	1182		
226	0245		
227	1213		
228	1242		

Table II. Sample set of counts versus time data taken from the analyzer output

Counts	Time(sec)	Counts	Time(sec)
20763	0	12947	2520
18038	120	13080	2720
18196	320	11278	2920
17364	520	12687	3120
16555	720	12815	3320
15686	920	12603	3520
15314	1120	12580	3720
14860	1320	12393	3920
14252	1520	12711	4120
13728	1720	12313	4320
13747	1920	11929	4520
13497	2120	12344	4720
13285	2320		

Table III. Sample set of normalized data with background subtracted used in the determination of D.

Normalized Counts	Time(sec)	Normalized Counts	Time(sec)
1.00000	0	.5521	2520
.8433	120	.5582	2720
.8524	320	.4546	2920
.8045	520	.5356	3120
.7580	720	.5430	3320
.7080	920	.5308	3520
.6866	1120	.5294	3720
.6605	1320	.4959	3920
.6256	1520	.5145	4120
.5955	1720	.4909	4320
.5965	1920	.4700	4520
.5822	2120	.4953	4720
.5700	2320		

the diffusion process. A normal distribution was assumed for errors in measurement of count rate while time measurements were assumed to have negligible error. The accuracy of a determination of the diffusion coefficient was decreased by these errors. Confidence limits on the individual diffusion coefficients were based upon the residues of the curve from which each D was determined. An explanation of the method employed is given in this section.

Given the relationship

$$X = f(t,D) \tag{32}$$

where D is a dependent variable of the measured quantities X and t, the error of D due to errors in measurement is given by the theory of propagation of errors. Letting D equal diffusion coefficient, t equal time, X equal normalized count rate, and variances of the quantities X, D, and t equal σ_x^2, σ_D^2, and σ_t^2, respectively, the relationship given is

$$\sigma_x^2 = \left(\frac{\partial f(t,D)}{\partial D}\right)^2 \sigma_D^2 + \left(\frac{\partial f(t,D)}{\partial t}\right)^2 \sigma_t^2. \tag{33}$$

Since σ_t^2 can be set equal to zero if the measurement of t has negligible error, the variance of D calculated from N data points is given as

$$\sigma_D^2 = \sigma_x^2 \left[\sum_{i=1}^{N} \left(\frac{\partial f(t,D)}{\partial D}\right)^2\right]^{-1}. \tag{34}$$

Using Eq. (34) and the "t test" it is possible to ascribe a confidence interval to the D value.

Brownlee (81) has presented a formula for an estimate of σ_x^2 based upon the residuals between the least squares fit and the data. The best estimate of the variance of X is given by

$$\sigma_x^2 = (N-c)^{-1} \sum_{i=1}^{N} (Xc_i - Xe_i)^2 \tag{35}$$

where (N-c) = number of degrees of freedom associated with σ_x^2

c = number of variables, which was one for this analysis.

Thus, from Eqs. (34) and (35) the standard deviation for D is

$$\sigma_D = \left\{(N-1)^{-1} \sum_{i=1}^{N} (Xc_i - Xe_i)^2 \left[\sum_{i=1}^{N} \left(\frac{\partial f(t,D)}{\partial D}\right)^2 \right]^{-1} \right\}^{1/2} \qquad (36)$$

A 67 percent confidence limit corresponding to one standard deviation was placed on the diffusion coefficient values by using the "t test" with the appropriate number of degrees of freedom. The diffusion coefficient was reported as

$$D \pm t^* \sigma_D$$

where t* was taken from a table of the "t" distribution.

3.0 RESULTS AND DISCUSSION

3.1 General Discussion

The purpose of this study was to demonstrate the feasibility of measuring diffusion coefficients with a tracer technique in a modified Ney-Armistead cell containing a semiconductor detector. The apparatus was used to measure diffusion coefficients in the transition diffusion regime because very little data exist for diffusion at pressures which cause transitional behavior to occur. Results given in this section illustrate the success of the experimental method employed. A sample set of raw data for a typical diffusion run are presented in Table III.

Experimentally determined self-diffusion coefficients in the transition pressure range for carbon dioxide at 20°C are presented in Table IV and Fig. 9. These results have been compared with theoretical values of D_e for Bosanquet's additive resistance law and Wheeler's empirical relationship given in Eqs. (16) and (17), respectively. Values of D_{11} used in the theoretical calculations were taken from the theory of Chapman and Cowling (see Eq. (7)) while those for D_k were calculated by Eq. (11). To simplify calculations, D_{11} was evaluated for p = 760 mm and T = 39.6°C and a knowledge of the inverse relationship between D_{11} and p and of the proportionality between D_{11} and $T^{3/2}$ was applied to the calculation of D_{11} at reduced temperatures and pressures. All diffusion data were taken at 20°C. The reported experimental values of D_e were calculated from Eq. (24) using experimental measurements of D_{12}, the diffusion coefficient of $C^{14}O_2$ in CO_2. Using the atomic masses 14.008 for C^{14}, 12.010 for C, and 16.000 for O, the correction factor was 1.011.

Table IV. Experimental and theoretical results for the self-diffusion coefficient of carbon dioxide in the transition pressure range

Run No	p Microns	$D_{e_{12}}$ (cm^2/sec) Experimental	D_e (cm^2/sec) Experimental self-diffusion	D_e (cm^2/sec) Bosanquet	D_e (cm^2/sec) Wheeler
1	10	868	878 ± 63	1085.5	1160.3
2	12	873	883 ± 110	1057.6	1143.3
3	16	982	993 ± 68	1005.6	1110.1
4	17	820	829 ± 52	993.6	1102.1
5	28	804	813 ± 50	876.8	1018.3
6	31	1111	1123 ± 109	849.6	997.0
7	36	1050	1062 ± 94	807.8	962.8
8	50	742	750 ± 68	710.0	875.5
9	52	782	791 ± 35	697.9	863.9
10	57	919	930 ± 81	669.4	936.0
11	64	641	648 ± 26	633.3	799.0
12	68	664	672 ± 27	614.3	778.9
13	86	763	772 ± 31	545.0	701.3
14	87	803	812 ± 34	537.8	693.0
15	90	584	591 ± 27	527.5	680.7
16	95	602	608 ± 22	511.0	661.0
17	99	611	618 ± 40	498.6	645.7
18	106	565	572 ± 22	478.3	620.4
19	123	608	615 ± 26	435.2	565.0
20	128	451	456 ± 25	423.9	550.1
21	161	469	474 ± 13	362.2	466.0
22	167	369	373 ± 8	352.9	452.9
23	167	326	329 ± 11	352.9	452.9
24	191	392	396 ± 8	319.9	406.4
25	210	319	323 ± 15	297.8	374.9
26	242	278	282 ± 7	266.8	330.7
27	260	283	286 ± 10	252.1	309.7
28	340	254	256 ± 7	202.4	240.1
29	409	213	215 ± 8	172.9	200.3
30	417	237	240 ± 22	170.1	196.5
31	477	201	203 ± 6	151.3	172.0

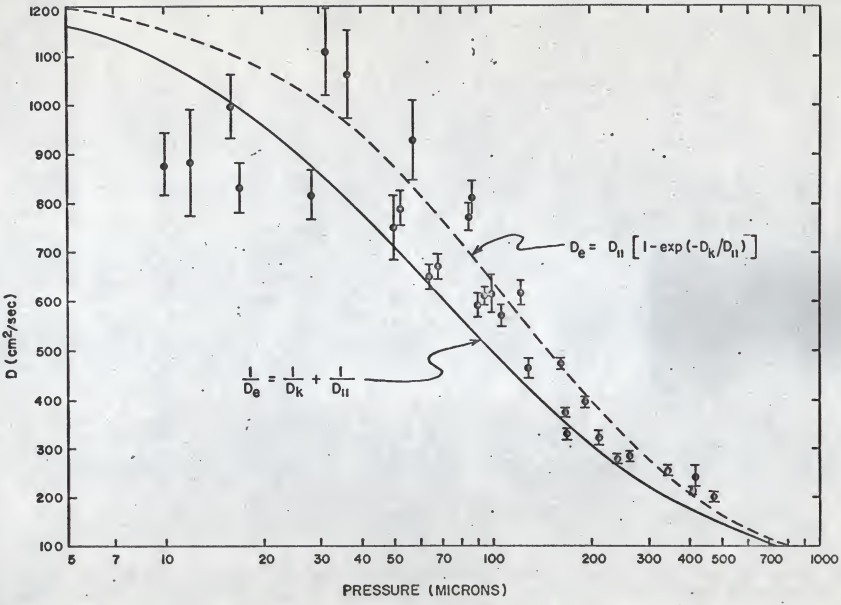

Fig. 9. Comparison between experimental and theoretical self-diffusion coefficients for CO_2.

The deviation reported for each experimental diffusion coefficient was the standard deviation which corresponds to 67% confidence limits. This deviation reflects the accuracy of the least squares fit of the data. It is not a complete measure of the accuracy of the diffusion coefficient, since as is shown subsequently, the accuracy of the diffusion coefficient for a selected pressure depends upon accuracy in the knowledge of pressure and certain system parameters. These standard deviations represent errors of approximately 3.5% at pressures higher than 50 microns and errors from 6 to 12% for data below 50 microns.

The degree of agreement between experiment and theory is shown in Fig. 9. At pressures greater than 40 microns experimental diffusion coefficients were in general well within the limits set by the theories of Bosanquet and Wheeler. Such observation is convincing evidence that this experimental technique offers promise as a research tool for the study of transition range diffusion. Four experimental values were less than those predicted by the additive resistance law at pressures of 10-30 microns, while two data points between 30 and 50 microns were larger than the expected values. It is noted that this scatter in the data occurs on the low pressure side of the transition range where Knudsen diffusion is predominant and the diffusion process is quite fast. This fact was used to explain the disagreement between experiment and theory over this range.

Most previous investigators suggest that Bosanquet's theoretical relationship gives the best estimate of transition range diffusion coefficients while others prefer Wheeler's empirical relationship. In view of this, one would expect close agreement between the theoretical curves presented and

the experimental data. Since no experimental D_{11} values for transitional self-diffusion of CO_2 in a diffusion cell with well defined geometry have been reported, it is impossible to compare these results with the work of others. The analysis of possible errors in measurement is discussed below.

Pressure control and measurement accounted for the largest single source of experimental error. As was discussed in section 2.5.1, accurate reading of the gauge dial was impossible and reproducibility of the gauge readings was no better than ± 10%. While the pressure measurement was not an input to the diffusion coefficient determination, it was used as the dependent variable in the functional relationship between D_{11} and p presented in Fig. 9. These factors could very well account for much of the scatter of D_{11} values above 50 microns. The absence of reproducibility and the possible presence of gauge tube drift at pressures below 20 microns might account for some error in the low D_{11} values for that range.

The technique applied to eliminate a pressure gradient in the diffusion cell after charging with the tracer gas is presented in Appendix C. Pressure readings in flask I at zero and "equilibrium" times indicated that for several runs a slight pressure gradient did exist. Any existing pressure gradient would have increased the measured diffusion coefficient. This effect was most likely at the higher pressures since more time would have been required to equalize the pressures by the technique employed. A facility for measuring the pressure in flask II would have been useful to prevent any question about the elimination of a pressure gradient.

The capillary tube valve used to prevent diffusion through the tube before the diffusion run was started did not provide a vacuum tight seal. It is possible that a measurable quantity of $C^{14}O_2$ diffused out of flask I

while the initial concentration was being measured. This would have caused a decrease in the measured diffusion coefficient. While it is unlikely that such an error would have been introduced at pressures above 50 microns, it is possible that this effect distorted measurements at lower pressures where diffusion through tiny openings is quite rapid. The surprisingly low values reported for D_{11} at pressures below 20 microns may be partially explained by this source of error. An additional explanation of these low values may be the statistical error in the radioactive count rate associated with the decrease in number of $C^{14}O_2$ molecules present at the lower pressures. The standard deviation for these diffusion coefficients illustrate the effect of reduced count rate. Both of these sources of error could be lessened by making a modified capillary valve and by using a trace gas with higher specific activity.

Calculations were performed on a set of theoretical concentration versus time data for L = 10.0 cm, R = 0.0513 cm and D = 95 cm^2/sec to demonstrate the effect of inaccurate volume and effective tube length measurements upon the measured diffusion coefficient. A 5 percent change in the theoretical tube length caused a corresponding change of 4 percent in the measured diffusion coefficient. A volume measurement of flask I in error by 2 percent (approximately 11 cc) caused a corresponding error in the diffusion coefficient of 2.4 percent. In measuring the volumes of the experimental flasks with water some error was probably introduced by the presence of flask side arms and the solid state detectors. These volume measurements could not have been in error by more than 5 cc (0.9 percent). The measured tube length was adjusted by applying the Rayleigh end-correction which is the accepted procedure for determining the effective tube length.

This correction does not allow for expected changes in the diffusion length as Knudsen diffusion becomes predominant. Presently no relationship exists for the change in effective tube length as a function of pressure.

It should be mentioned that the presence of trace gas in flask II at time zero required an adjustment in the data obtained to make it satisfy the mathematical model. The adjustment consisted of subtracting a background count from all count rate measurements. It was believed that this operation did not affect the results.

3.2 Conclusion

The discussion and results presented above have shown the advantages and disadvantages of this experimental apparatus. Based upon the results it is possible to arrive at several conclusions concerning the use of this experimental technique.

The feasibility of using a semiconductor detector in a modified Ney-Armistead diffusion cell to measure diffusion coefficients has been demonstrated. While the measurements taken were designed primarily to perform a feasibility study of the experimental method, transition range diffusion coefficients for CO_2 were found to compare within 10 percent at pressures from 50 to 400 microns with the theories of Bosanquet and Wheeler. This fact suggests that refinement of the apparatus will produce a useful research tool to be used in studying the mechanism of diffusion in the transition pressure range. As has been discussed previously, the present day need for such a device is great.

4.0 SUGGESTIONS FOR FURTHER STUDY

A first extension of this study would be to modify the diffusion cell as suggested in section 3.0. This would include the installation of a tighter valve on the capillary tube and a pressure gauge in flask II. It would be advisable to use high precision pressure gauges in order to get the most accurate pressure measurements possible. The flask volumes should be measured with a gas instead of a liquid and the constant temperature control should be improved to within $\pm$ 0.01^{o}C. If smaller bore capillary tubes are used the diameter should be determined by optical or viscosity measurements.

Since the technique for removing a pressure gradient across the capillary tube caused radioactive gas to enter flask II, the data had to be modified to fit the mathematical model. The one-dimensional diffusion equation should be re-solved for the same boundary conditions modified to include the assumption of an initial concentration in flask II. The use of two detectors, one in each flask, and a new mathematical model ignoring the tube volume would simplify the reduction of data and allow several diffusion measurements during one run, but greatly complicate the electronics.

After improving the accuracy of this experimental method, self-diffusion coefficients could be determined as a function of pressure or temperature for many gases, e.g., surfur dioxide, methane and other hydrocarbons. The measurement of binary diffusion coefficients and the study of simultaneous pressure and concentration gradient diffusion could be accomplished without modification of the experimental apparatus. Transitional flow parameters have been measured for only a very few gases. By changing the capillary tube it would

be possible to determine the effect of the tube length upon the measurement of the diffusion coefficients. Such a study might lead to an understanding of the mechanism for diffusion in the transition pressure range. By the use of multiple tracers, future work could include the study of ternary diffusion.

5.0 ACKNOWLEDGMENT

The author wishes to express his gratitude to Dr. J. O. Mingle for originating this study and for inviting his participation. Sincere thanks are extended also to Dr. J. O. Mingle for his guidance, helpful suggestions and constructive criticism throughout the course of this study. Sincere appreciation is given to Dr. W. R. Kimel for his assistance and guidance. The Kansas State University Engineering Experiment Station and the Petroleum Research Fund of the American Chemical Society are thanked for their financial support.

6.0 LITERATURE CITED

1. Adzumi, E.
   Bull. Chem. Soc. Japan, 12,199, (1957).

2. Amdur, I. and T. F. Schatzki
   Diffusion Coefficients of Systems Xe-Kr and A-Xe. J. Chem. Phys., 27, 1049, (1957).

3. Amdur, I., J. W. Irvine, Jr., E. A. Mason, and J. Ross
   Diffusion Coefficients of Systems CO_2-CO_2 and CO_2-N_2O. J. Chem. Phys., 20, 436, (1952).

4. Bendt, Phillip J.
   Measurements of He^3-He^4 and H_2-D_2 Gas Diffusion Coefficients. Phys. Rev., 110, 85, (April, 1958).

5. Bird, R. B., W. E. Stewart, and E. N. Lightfoot
   Transport Phenomena. New York: John Wiley & Sons, Inc., (1960).

6. Blankenship, J. L.
   Bibliography on Semiconductor Nuclear Radiation Detectors. ORNL-2583, (April, 1962).

7. Blankenship, J. L., and C. J. Borkowski
   Silicon Surface Barrier Nuclear Particle Spectrometer. Proceedings of the 7th Scintillation Counter Symposium, Washington, DC, (1960).

8. Boardman, L. E. and N. E. Wild
   The Diffusion of Pairs of Gases with Molecules of Equal Mass. Proc. Roy. Soc. (London), 162A, 511, (1937).

9. Bosanquet, C. H.
   British TA Report. BR - 507, (Sept., 1944).

10. Boyd, Charles, Norman Stein, Virginia Steingrimsson, and William R. Rumpel
    An Interferometric Method of Determining Diffusion Coefficients in Gaseous Systems. J. Chem. Phys., 19, 548, (1951).

11. Brown, C. C.
    Solid State Radiation Detectors. Nuclear Science, IRE Transactions on Nuclear Science, 8, 331, (Jan., 1961).

12. Brownlee, K. A.
    Statistical Theory and Methodology in Science and Engineering. Second Edition. New York: John Wiley & Sons, Inc., (1965).

13. Buckingham, E.
    U. S. Dept. Agr., Bur. Soils, Bull. No. 25, (1904).

14. Carman, P. C.
Flow of Gases Through Porous Media. London: Butterworth Scientific Publications, (1956).

15. Carmichael, L. T., H. H. Reamer, B. H. Sage, and W. N. Lacey
Diffusion Coefficients in Hydrocarbon System. Ind. Eng. Chem., 4, 2205, (Oct., 1955).

16. Chapman, Sidney, and T. G. Cowling
Mathematical Theory of Non-uniform Gases. Second Edition. Cambridge: Cambridge University Press, (1952).

17. Chen, N. J. and D. F. Othmer
New Generalized Equation for Gas Diffusion Coefficient. Journal of Chemical and Engineering Data, 7, 1, (Jan., 1962).

18. Coward, H. F. and E. H. M. Georgeson
The Diffusion Coefficient of Methane and Air. J. Chem. Soc., 2, 1085, (1937).

19. Crank, J.
The Mathematics of Diffusion. Oxford: Claredon Press, (1956).

20. Crawford, G. E.
Semiconductors as Radiation Detectors. Nuclear Power, 4, 84, (Aug., 1959).

21. Curtiss, Charles F. and Joseph O. Hirschfelder
Transport Properties of Multicomponent Gas Mixtures. J. Chem. Phys., 17, 550, (June, 1949).

22. Daniels, F., J. H. Mathews, J. W. Williams, P. Bender, and R. A. Alberty
Experimental Physical Chemistry. New York: McGraw-Hill Book Company, (1956).

23. Dearnaley, G. and N. C. Northrop
Semiconductor Counters for Nuclear Radiations. New York: John Wiley & Sons, Inc., (1963).

24. De Marcus, W. C.
The Problems of Knudsen Flow. Parts I-V. K-1302, (Sept., 1956).

25. DeMarcus, W. C.
Knudsen Flow Through a Channel with Rough Walls. K - 1435, (Oct., 1959).

26. Dushman, Saul
Scientific Foundation of Vacuum Techniques. New York: John Wiley & Sons, Inc., (1962).

27. Eberhardt, W. H.
On Gaseous Self-Diffusion in Capillaries K-1401, (April, 1959).

28. Estermann, J.
Techniques of Measurement in Rarefied Gases. Rarefied Gas Dynamics, International Series on Aeronautical Sciences and Space Flight, Division IX: Symposia, 3, 38, (1960).

29. Evans, R. B. III, J. Truitt, and G. M. Watson
Superposition of Forced and Diffusive Flow in a Large-Pore Graphite. ORNL-3067, (March, 1961).

30. Evans, R. B. III, G. M. Watson, and E. A. Mason
Gaseous Diffusion in Porous Media at Uniform Pressure. J. Chem. Phys., 35, 2076-2083, (Dec., 1961).

31. Fairstein, E. and J. Hahn
Nuclear Pulse Amplifiers - Fundamentals and Design Practice. Nucleonics, 23, 56, (July, 1956).

32. Friend, Leo, and Stanley B. Adler
Transport Information Needed in the Chemical and Process Industries. Transport Properties in Gases. Evanston, Ill.: Northwestern University Press, (1957).

33. Gaede, W.
Ann. Physik, 41, 289, (1913).

34. Giddings, J. Calvin, and Spencer L. Seager
Method for Rapid Determination of Diffusion Coefficients. Industrial and Engineering Chemistry Fundamentals, 1, 277, (1960).

35. Goulding, F. S.
Semiconductor Detectors - Their Properties and Applications. Nucleonics 22, 54, (May, 1964).

36. Groth, W. and P. Harteck
Z. Electrochemi, 47, 167, (1941).

37. Guthrie, Andrew
Vacuum Equipment and Techniques. New York: McGraw-Hill Book Company, (1949).

38. Harteck, P. and H. W. Schmidt
Z. Physik, Chem., 21B, 447, (1932).

39. Hartley, G. S. and J. Crank
Some Fundamental Definitions and Concepts in Diffusion Processes. Trans. Faraday Soc., 45, 801, (1949).

40. Harris, D. D.
Numerical Methods Using Fortran. Columbus, Ohio: Charles E. Merrill

Books, Inc., (1964).

41. Hildebrand, F. B.
Introduction to Numerical Analysis. New York: McGraw-Hill Book Company, (1956).

42. Hirschfelder, J. O., C. F. Curtiss, and R. B. Bird
Molecular Theory of Gases and Liquids. New York: John Wiley & Sons., Inc., (1954).

43. Hofstadter, R.
Crystal Counters. Part I. Nucleonics, 4, (April, 1949).

44. Hofstadter, R.
Crystal Counters, Part II. Nucleonics 4, (May, 1949).

45. Hougen, Olaf A.
Engineering Aspects of Solid Catalysts. Ind. Eng. Chem., 53, 509, (July, 1961).

46. Hutchinson, Franklin
Self Diffusion in Argon. J. Chem. Phys., 17, 1081, (1941).

47. Hutchinson, Franklin
Phys. Rev., 72, 1256, (1947).

48. Jeffries, Q. R. and H. G. Drickamer
Diffusion in CO_2-CH_4 Mixtures to 225 Atm. J. Chem. Phys., 22, 436, (March, 1954).

49. Johnson, E. F.
Molecular Transport Properties of Fluids. Ind. Eng. Chem., 45, 902, (May, 1953).

50. Johnson, E. F.
Molecular Transport Properties of Fluids. Ind. Eng. Chem., 47, 599, (March, 1955).

51. Johnson, E. F.
Molecular Transport Properties of Fluids. Ind. Eng. Chem., 48, 582, (1956).

52. Kennard, Earle H.
Kinetic Theory of Gases. New York: McGraw-Hill Book Company, (1938).

53. Knudsen, Martin
Kinetic Theory of Gases. Third Edition. New York: John Wiley & Sons Inc., (1950).

54. Kohl, Jerome, Rene D. Zentner, and Herbert R. Lukens
Radioisotope Applications Engineering. Princeton: D. Van Nostrand Company, Inc., (1961).

55. Lee, C. Y. and C. R. Wilke
Ind. Eng. Chem., 46, 2381-2387, (1954).

56. Liley, P. E.
Survey of Recent Work on Viscosity, Thermal Conductivity and Diffusion of Gases. Progress in International Research in Thermodynamics and Transport Properties, New York: McGraw-Hill Book Company, (1959).

57. Loschmidt, J.
Sitzb. Akad. Wiss. Wien., 61, 367, (1870).

58. Maxwell, J. C.
Electricity and Magnetism. Oxford: Oxford University Press, (1892).

59. Ney, Edward P. and Fontaine C. Armistead
The Self-Diffusion Coefficient of Uranium Hexafluoride. Phys. Rev., 71, 14, (Jan., 1947).

60. O'Hern, H. A. and Joseph J. Martin
Diffusion in CO_2 at Elevated Pressures. Ind. Eng. Chem., 47, 2081, (1955).

61. Opfell, J. B. and B. H. Sage
Application of Least Squares Method. Ind. Eng. Chem., 50, 803, (1958).

62. Otani, Seiya, N. Wakao, J. M. Smith
Diffusion and Flow in Porous Catalysts. A. I. Ch. E. Journal, 11, 439.

63. Patterson, G. N.
Molecular Flow of Gases. New York: John Wiley & Sons, Inc., (1956).

64. Paul, Ranjit
Solutions of Concentration Dependent Diffusion Equation. Phys. Fluids, 3, (1960).

65. Pollard, W. G. and R. D. Present
On Gaseous Self Diffusion in Long Capillary Tubes. Phys. Rev., 73, 762, (April, 1948).

66. Present, R. D.
Kinetic Theory of Gases. New York: McGraw-Hill Book Company, (1958).

67. Price, W. J.
Nuclear Ridiation Detection. Second Edition. New York: McGraw-Hill Book Company, (1964).

68. Radeka, Veljko
Low Noise Preamplifiers for Nuclear Detectors. Nucleonics, 23, 52, (July, 1965).

69. Reamer, H. H. and B. H. Sage
The Measurement of Diffusion Coefficients in Gases and Liquids at Elevated Temperatures. Transport Properties in Gases. Evanston, Ill: Northwestern University Press, (1958).

70. Rothfeld, Leonard B.
Gaseous Counterdiffusion in Catalyst Pellets. A. I. Ch. E. Journal, 9, 19, (Jan., 1963).

71. Schaaf, Samuel A. and Paul L. Chambre
Flow of Rarefied Gases. Fundamentals of Gas Dynamics. Princeton: Princeton University Press, (1961).

72. Scintillators and Semiconductors. Nucleonics, 18, 85, (1960).

73. Scott, D. S. and F. A. L. Dullien
Diffusion of Ideal Gases in Capillaries and Porous Solids. A. I. Ch. E. Journal, 8, 113, (March, 1962).

74. Semiconductors, Scintillators, and Pulse-Height Analyzers. Nucleonics, 20, 53, (May, 1962).

75. Sharpe, Jack
Nuclear Radiation Detectors. Second Edition. New York: John Wiley & Sons., Inc., (1964).

76. Sherman, F. S.
Transport Phenomena in Low-Density Gases. Transport Properties in Gases. Evanston, Ill: Northwestern University Press, (1958).

77. Strehlow, Roger A.
The Temperature Dependence of the Mutual Diffusion Coefficient for Four Gaseous Systems. J. Chem. Phys., 21, 2101, (1953).

78. Strutt, J. W. (Lord Rayleigh)
Theory of Sound. New York: Dover Publications, (1945).

79. Taylor, Angus E.
Advanced Calculus. New York: Ginn & Company, (1955).

80. Taylor, J. M.
Semiconductor Particle Detectors. Washington, D. C.: Butterworth, (1963).

81. Timmerhaus, K. D. and H. G. Drickamer
Self-Diffusion in CO_2 at Moderate Pressure. J. Chem. Phys., 19, 1242-1243, (1951).

82. Tordai, L.
Errors in Diffusion Measurements by the Loschmidt Method. Br. J. Appl. Phys., 1, 329, (1950).

83. Visner, Sidney
Self Diffusion in Capillaries at Low Pressures. Phys. Rev., 82, 57, (1951).

84. Wakao, N. and J. M. Smith
Diffusion in Catalyst Pellets. Chemical Engineering Society, 17, 825, (1962).

85. Wakao, N., Sevia Otani, and J. M. Smith
Significance of Pressure Gradients in Porus Material. Part I. A. I. Ch. E. Journal, 11, 435, (May, 1965).

86. Westenberg, A. A. and R. E. Walker
Experiments in the Molecular Diffusion of Gases at High Temperatures. Thermodynamic and Transport Properties of Gases, Liquids and Solids. New York: McGraw-Hill Book Company, (1959).

87. Wheeler, A.
Advances in Catalysis. New York: Academic Press, (1951).

88. Winn, E. B.
The Self-Diffusion Coefficient of Nitrogen, Phys. Rev., 74, 689, (1948).

89. Winn. E. B.
The Temperature Dependence of the Self-Diffusion Coefficients of Argon, Neon, Nitrogen, Oxygen, Carbon Dioxide and Methane. Phys. Rev., 80, 1024, (1950).

90. Winn, E. B. and E. P. Ney
The Determination of the Self-Diffusion Coefficient of Methane. Phys. Rev., 72, 77, (1947).

91. Winter, E. R. S.
Diffusion Properties of Gases. Part IV. The Self-Diffusion Coefficients of Nitrogen, Oxygen, and Carbon Dioxide. Trans. Faraday Soc., 47, 342, (1951).

92. Wylie, C. R.
Advanced Engineering Mathematics. Second Edition. New York: McGraw-Hill Book Company, (1960).

7.0 APPENDICES

7.1 APPENDIX A

Solution to the Differential Equation for Diffusion Through a Capillary Tube

Based upon the assumption that Fick's second law is valid for the process of gaseous diffusion in a capillary tube, the partial differential equation which described gaseous diffusion in the system under study was

$$\frac{\partial C}{\partial t} = D \frac{\partial^2 C}{\partial z^2} . \tag{A-1}$$

In this section, Eq. (A-1) is solved by the method of Laplace transforms (92) for the three following boundary conditions:

$$t = 0,\ z>0,\ C = 0 \tag{A-2}$$

$$t>0,\ z = 0,\ C\Big|_{z=0} = C_o - V_1^{-1} \int_0^t -D\pi R^2 \frac{\partial C}{\partial z}\Big|_{z=0} dt \tag{A-3}$$

$$t>0,\ z = L,\ C\Big|_{z=L} = C_o V_1 V_2^{-1} - CV_1 V_2^{-1}\Big|_{z=0} - V_2^{-1} \int_0^L C\pi R^2 dz. \tag{A-4}$$

To transform Eq. (A-1) and the boundary conditions to dimensionless equations let $X = C/C_o$, $\xi = z/L$, and $\tau = tD/L^2$. These definitions, when applied to the format of Eqs. (A-1), (A-2), (A-3), and (A-4), yield

$$\frac{\partial X(\tau,\xi)}{\partial \tau} = \frac{\partial^2 X(\tau,\xi)}{\partial \xi^2} , \tag{A-5}$$

while the boundary conditions become

$$\tau = 0,\ \xi>0,\ X = 0 \tag{A-6}$$

$$\tau>0,\ \xi = 0,\ X = 1 - \alpha \int_0^\tau \frac{\partial X(\tau,0)}{\partial \xi} d\tau \tag{A-7}$$

$$\tau>0,\ \xi = 1,$$

$$X(\tau,1) = -\beta\left\{\int_0^{\tau} \frac{\partial X(\tau,0)}{\partial \xi} d\tau - \int_0^1 X(\tau,\xi)d\xi\right\} \tag{A-8}$$

where $\beta = \pi R^2 L V_2^{-1}$ and $\alpha = \pi R^2 L V_1^{-1}$.

Equation (A-5), with the accompanying boundary conditions (A-6), (A-7), and (A-8), is transformed with respect to the independent variable τ, thus letting

$$\mathcal{L}\left[X(\tau,\xi)\right] = X(s,\xi),$$

and using Eq. (A-6), Eq. (A-5) becomes

$$sX(s,\xi) = \frac{d^2X(s,\xi)}{d\xi^2}\ . \tag{A-9}$$

Solving this ordinary second order differential equation, it is found that

$$X(s,\xi) = A(s)\ \sinh(\lambda\xi) + B(s)\ \cosh(\lambda\xi) \tag{A-10}$$

where $\lambda = s^{1/2}$.

To determine the coefficient functions A(s) and B(s) it is observed that the Laplace transforms of boundary conditions (A-7) and (A-8) are

$$\tau>0,\ \xi = 0,\ X(s,0) = s^{-1} + \alpha s^{-1}\ \frac{dX(s,0)}{d\xi}\ . \tag{A-11}$$

and

$$\tau>0,\ \xi = 1,\ X(s,1) = -\beta s^{-1}\ \frac{dX(s,0)}{d\xi} - \beta\int_0^1 X(s,\xi)d\xi. \tag{A-12}$$

Taking the derivative of Eq. (A-10) and applying boundary condition (A-11),

$$B(s) = s^{-1} + s^{-1}\ \frac{dX(s,0)}{d\xi}$$

$$= s^{-1} + \alpha s^{-1}\left[A(s)\lambda\ \cosh(0) + B(s)\ \sinh(0)\right] \tag{A-13}$$

thus

$$B(s) = s^{-1} + \alpha A(s)\lambda^{-1}. \tag{A-13A}$$

Applying boundary condition (A-12) to Eq. (A-10)

$$A(s)\sinh(\lambda 1) + (s^{-1} + \alpha A(s)\lambda^{-1})\cosh(\lambda 1) =$$

$$-\beta A(s)\lambda^{-1} - \beta\int_0^1 \left[A(s)\sinh(\lambda\xi) + (s^{-1} + \alpha A(s)\lambda^{-1}\cosh(\lambda\xi)\right] d\xi. \tag{A-14}$$

After performing the indicated integration and simplification of Eq. (A-14), the coefficient function A(s) is found to have the form

$$A(s) = -\lambda^{-1}(\lambda\cosh\lambda + \beta\sinh\lambda)\left[(\alpha\beta + s)\sinh\lambda + (\alpha\beta + \beta\lambda)\cosh\lambda\right]^{-1}. \tag{A-15}$$

Substituting the expressions for A(s) and B(s) into Eq. (A-10) and simplifying gives the solution for $X(s,\xi)$ as a function of the variables s and ξ as follows:

$$X(s,\xi) = s^{-1}\cosh(\lambda\xi)$$

$$-\{s^{-1}(\lambda\cosh\lambda + \beta\sinh\lambda)(\lambda\sinh(\lambda\xi) + \alpha\cosh(\lambda\xi))$$

$$\left[(\alpha\beta + s)\sinh\lambda + (\alpha + \beta)\lambda\cosh\lambda\right]^{-1}\}. \tag{A-16}$$

In order to use one of Heaviside's expansion theorems in finding the inverse of Eq. (A-16), it is necessary to find the unrepeated roots of both the first and second terms of the equation. Clearly, zero is a root of both terms and only the second term has non-zero roots of higher order. These roots are found by equating the denominator of the second term to zero as follows:

$$s\left[(\alpha\beta + s)\sinh\lambda + (\alpha + \beta)\lambda\cosh\lambda\right] = 0 \tag{A-17}$$

which leads to the expression

$$\tanh \lambda_n = - \lambda_n(\alpha + \beta)/(\alpha\beta + \lambda_n^2). \tag{A-18}$$

Equation (A-18) has an infinite number of imaginary roots designated by λ_n.

Finding the inverse of Eq. (A-16) by Heaviside's formula using the roots given above yields

$$X(\tau,\xi) = \mathcal{L}^{-1}\left[\begin{matrix}\text{1st term}\\ \text{zero root}\end{matrix}\right] + \mathcal{L}^{-1}\left[\begin{matrix}\text{2nd term}\\ \text{zero root}\end{matrix}\right] + \mathcal{L}^{-1}\left[\begin{matrix}\text{2nd term}\\ \text{negative roots}\end{matrix}\right] \tag{A-19}$$

where

$$\mathcal{L}^{-1}\left[\begin{matrix}\text{1st term}\\ \text{zero root}\end{matrix}\right] = 1 \tag{A-20}$$

$$\mathcal{L}^{-1}\left[\begin{matrix}\text{2nd term}\\ \text{zero root}\end{matrix}\right] = \theta/\phi\Big|_{\lambda^2 = 0} \tag{A-21}$$

where

$$\theta = -(\lambda \cosh \lambda + \beta \sinh \lambda)(\lambda \sinh(\lambda\xi) + \alpha \cosh(\lambda\xi))e^{\lambda^2\tau}$$

$$\phi = (\alpha\beta + \lambda^2)\sinh \lambda + \lambda(\alpha + \beta)\cosh \lambda$$

$$+ \lambda^2\left[(2\lambda)^{-1}(\alpha\beta + \lambda^2 + \alpha + \beta)\cosh \lambda + (1/2(\alpha + \beta)+1)\sinh \lambda\right] \tag{A-22}$$

so that

$$\theta/\phi = - \alpha(1 + \beta)/(\alpha\beta + \alpha + \beta)$$

$$\mathcal{L}^{-1}\left[\begin{matrix}\text{2nd term}\\ \text{negative roots}\end{matrix}\right] = - \sum_{n=1}^{\infty} \theta^*_n/\phi^*_n \tag{A-23}$$

where

$$\theta^*_n = \lambda_n(\cosh \lambda_n + \beta \sinh \lambda_n)(\lambda_n \sinh(\lambda_n\xi) + \alpha \cosh(\lambda_n\xi))e^{\lambda^2\tau},$$

$$\phi_n^* = \lambda_n^2 \left[(2\lambda n)^{-1} (\alpha + \beta + \alpha\beta + \lambda_n^2) \cosh \lambda_n \right.$$

$$\left. + (1/2(\alpha + \beta) + 1) \sinh \lambda_n \right] .$$

Equation (A-23) is simplified by redefining λ_n^2 to have a positive value. This operation requires the substitution of $-\lambda_n^2$ for λ_n^2 in Eqs. (A-18) and (A-23). Using the identities

$$\tanh ix = i \tan x,$$

$$\cosh ix = \cos x,$$

$$\sinh ix = i \sin x,$$

and the definition for λ_n^2, causing λ_n to equal $i\lambda_n$, Eqs. (A-18) and (A-23) reduce to

$$\tan \lambda_n = - \lambda_n (\alpha + \beta) / (\alpha\beta - \lambda_n^2) \qquad \text{(A-24)}$$

and

$$\mathcal{L}^{-1} \left[\begin{array}{l} \text{2nd term} \\ \text{negative roots} \end{array} \right] = - \sum_{n=1}^{\infty} \theta_n^+(\lambda_n, \xi, \tau) / \phi_n^+(\lambda_n, \xi, \tau) \qquad \text{(A-25)}$$

where

$$\theta_n^+(\lambda_n, \xi, \tau) = e^{-\lambda_n^2 \tau} \left[\alpha \cos(\lambda_n \xi) - \lambda_n \sin(\lambda_n \xi) \right]$$

$$\left[\lambda_n \cos \lambda_n + \beta \sin \lambda_n \right]$$

$$\phi_n^+(\lambda_n, \xi, \tau) = \lambda_n^2 \left\{ (2\lambda_n)^{-1} (\alpha + \beta + \alpha\beta - \lambda_n^2) \cos \lambda_n \right.$$

$$\left. - \left[1/2(\alpha + \beta) + 1 \right] \sin \lambda_n \right\} .$$

The eigenvalues λ_n of Eq. (A-24) are solved accurately by Newton's method (41) given a close approximation to the actual λ_n values. The first order solution λ_1 is given by

$$\tan \lambda_1 \simeq \lambda_1 = \lambda_1(\alpha + \beta)/(\lambda_1^2 - \alpha\beta)$$

so that $\lambda_1 \simeq (\alpha + \beta + \alpha\beta)^{1/2}$.

Approximations to higher order values of λ_n are obtained by use of the algorithm $\lambda_n \simeq \lambda_{n-1} + \pi$.

Thus the solution to the partial differential equation (A-5), given by Eq. (A-19), can be written

$$X(\tau,\xi) = \beta/(\alpha + \beta + \alpha\beta) - \sum_{n=1}^{\infty} \phi_n^{\dagger}(\lambda_n,\xi,\tau)\phi_n^{\dagger}(\lambda_n,\xi,\tau) \qquad \text{(A-26)}$$

where λ_n^2 is a solution to the transcendental equation (A-24). Equation (A-26) shows the change in concentration gradient at a distance variable point z with respect to time as a function of the system parameters V_1,V_2, R,L, and D.

7.2 APPENDIX B

Experimental Procedure

Several preparatory operations were necessary to insure a knowledge of the conditions existing upon the diffusion cell (37). The constant temperature bath was set to maintain a constant temperature (20°C) by adjusting the thermoregulator to the appropriate setting. It was observed that the control maintained the desired temperature with variations of ± 0.5°C. After carefully installing the surface-barrier detector the system was outgassed with all valves except "9" open (See Fig. 4). Three days of outgassing caused the pressure increase with stopcock "13" closed, due to leakage and desorption of gases from the system walls, to be less than 0.1 microns per four hour period at a pressure of 1 micron. With the $C^{14}O_2$ charging flask "1" evacuated, stopcock "2" and needle valve "3" were closed. The charging flask containing the ampoule of $C^{14}O_2$ was removed, the ampoule tip was broken with a short glass rod housed in the charging flask, and the flask was again connected to the vacuum system. The system was purged with CO_2 and evacuated to 15 microns four times before beginning the thermocouple vacuum gauge calibration. This calibration was performed by charging the diffusion cell with CO_2, evacuating to the desired pressure, closing stopcock "13", and allowing 10 minutes for the system to reach an equilibrium pressure throughout before the pressure was measured with the McLeod gauge (26). Calibration data points were taken from 1 to 500 microns and used to construct a calibration curve for the thermocouple gauge. Each day before operating the diffusion cell the vacuum system was checked for leaks

and periodically the calibration was "spot" checked to determine whether or not the thermocouple gauge was drifting. No drift was noticed if the gauge was turned on at least one hour before operating, but the reproducibility of the pressure readings varied considerably when the system was alternately charged and evacuated.

It was necessary to use a well-regulated power source for the amplifiers, the detector bias supply, the reverse bias discriminator, the time base generator, and the multichannel analyzer to remove transients and ground loop noises from the electronics system. When installing the electronics all plug ground lines were connected to receptacle ground lines and a small grounded copper cable was soldered to each component chassis. The diffusion cell was charged with CO_2 and evacuated to approximately 200 microns before slowly raising the detector bias voltage. To determine the proper detector bias setting the oscilloscope and microammeter were employed while the preamplifier was set for x6 amplification, the main and post amplifiers for x4, and the discriminator for 0.0 volts discrimination. The noise signal had an amplitude of several volts and a frequency of 120 cycles/sec before the electrical shield was placed around flask I housing the detector (See Fig. 2). The minimum noise signal was then found to occur at a detector bias setting of 50 volts. This noise signal could be totally removed by a discriminator setting of 0.21. The frequency of the square wave used to trigger the channel advance was calibrated with a stopwatch.

The actual diffusion data was taken by performing the following steps:

1. The system was evacuated to less than 1 micron and needle valve "3" closed. Stopcock "14" was closed while the system was purged with CO_2 through stopcock "9" three times and evacuated to the

desired pressure for the diffusion measurement.

2. Stopcock "13" was closed. After the gas reached equilibrium in the flasks the capillary valve "10" was closed and stopcock "2" was cracked momentarily to allow radioactive gas to fill the volume between "2" and "3". The capillary valve "10" was positioned by centering the ground glass joint handle between three stationary reference points.
3. The frequency of the square wave was set to a predetermined rate appropriate to the gas pressure in the flasks. This varied between 0.2 and 0.025 cycles per second. With the preamplifier, main and post amplifiers set at x6, x4, and x4, respectively, the detector bias was applied and all background counts eliminated by observing the oscilloscope and changing the discriminator adjustment. The correct discriminator setting varied between 0.19 and 0.24.
4. All electronic settings, the pressure of the gas, and the temperature of the water were recorded.
5. With stopcock "4" open, radioactive carbon dioxide was throttled slowly into flask I. At the instant pulses were observed on the oscilloscope, stopcock "4" and the needle valve were closed. After a period of approximately 10 seconds, stopcocks "11", "5", and "12" were closed, the pressure was noted, and the multichannel analyzer and a stopwatch were started. After allowing several scaling channels to collect counts without diffusion occurring, the capillary valve was opened and the time noted.
6. After counts were recorded in all 256 channels, the digital printer

automatically printed each channel number with its corresponding number of counts on a paper tape. Using the visual display of the analyzer it was possible to evaluate the apparent reliability of the data and whether or not equilibrium conditions had been reached. Another trace of the activity as a function of time was provided for those runs in which equilibrium had not been reached. The final gas, pressure, and water temperature were recorded after stopcocks "5", "11", and "12" were opened.

7.3 APPENDIX C

Data Analysis for the Diffusion Coefficient

The values of the diffusion coefficient for each run were determined by finding the least squares fit of a mathematical representation of the diffusion process to the concentration versus time data. The solution (see Eq. 30) to the diffusion equation which described the process occurring in the diffusion cell was nonlinear in D; consequently, it was necessary to employ an iterative procedure in determining the least squares fit of the data. The application of least squares analysis to the data, the numerical approximations utilized in constructing the computer program, and the computer program used to perform the iterations are discussed in the following paragraphs.

7.3.1 Least Squares Analysis and Numerical Approximations

In the method of least squares (99) the sum of the squares of deviations, Re, between the observed values, Xe_i, and the predictions, Xc_i, are minimized to find the values of Xc_i which give the minimum error. Applying this method of analysis to the diffusion data the expression for the residue, Re, is

$$Re = \sum_{i=1}^{N} (Xe_i - Xc_i)^2 \qquad (C\text{-}1)$$

where Xe_i and Xc_i are the i^{th} experimental and calculated values of X^* at

---

* See Nomenclature, p. vi.

time t_i respectively, and N is the number of data points. The minimum squared error is found by differentiating Re with respect to D and setting the resultant equal to zero; thus,

$$\frac{\partial Re}{\partial D} = -2 \sum_{i=1}^{N} (Xe_i - Xc_i) \frac{\partial Xc_i}{\partial D} = 0. \tag{C-2}$$

Setting f_D equal to $\frac{\partial Re}{\partial D}$ after dividing through by minus two and approximating f_D by the first two terms of a Taylor's series expansion (82) the result is

$$f_D = f_{D_o} + \overline{\Delta D} \frac{\partial f_D}{\partial D} \tag{C-3}$$

and where f_D should be zero by Eq. (C-2) so that

$$\overline{\Delta D} = -f_{D_o} \left[\frac{\partial f_D}{\partial D} \right]^{-1}. \tag{C-4}$$

To evaluate the right hand member of Eq. (C-4) use

$$\frac{\partial f_D}{\partial D} = \sum_{i=1}^{N} \left[(Xe_i - Xc_i) \frac{\partial^2 Xc_i}{\partial D^2} - \left(\frac{\partial Xc_i}{\partial D}\right)^2 \right] \tag{C-5}$$

where

$$\frac{\partial Xc_i}{\partial D} = \sum_{i=1}^{N} (\lambda_n^2 \tau / L^2) \theta_n^{\dagger}(\lambda_n, \xi, \tau) / \phi_n^{\dagger}(\lambda_n, \xi, \tau) \tag{C-6}$$

$$\frac{\partial^2 Xc_i}{\partial D^2} = -\sum_{i=1}^{N} (\lambda_n^2 \tau / L^2)^2 \theta_n^{\dagger}(\lambda_n, \xi, \tau) / \phi_n^{\dagger}(\lambda_n, \xi, \tau). \tag{C-7}$$

The value of D with minimum error can be determined by using the algorithm $D_{n+1} = D_n + \overline{\Delta D}$ and iterating upon D until $\overline{\Delta D}$ is sufficiently small.

7.3.2 Computer Program

The least squares analysis was performed by using an IBM-1410 computer. The program was written in FORTRAN IV(83) and required approximately ten minutes of computer time to yield a solution. A symbol table (see Table III) and the object program containing explanatory comment statements are presented in this section. The main program, DATA ANALYSIS, which performed the least squares analysis and one subroutine, XCALC, which computed Xe_i constitute the two major divisions of the program.

Table V. Symbols used in the least squares fit of the data

Symbol	Meaning
NSETS	Number of sets of data
NDATA	Numbers of data points in a set
Z	Distance variable along tube, Z
R	Radius of capillary tube, R
XLO	Effective length of capillary, tube, L
XDO	Diffusion coefficient, D
V1	Volume of flask I
V2	Volume of flask II
ERR1	Error criterion for main program
ERR2	Error criterion for subprogram
XEXP(K)	Normalized experimental count rate at data point K
T(K)	Time associated with data point K
XC(1,1,J)	Xc_i for XL(1) and XD(1) at time T(J) where J equals i
PXCD(J)	Partial derivative of Xc_i with respect to D when J equals i
PXCDD(J)	Second partial derivative of Xc_i with respect to D when J equals i
XDIF(J)	Difference between experimental and calculated values
RSIDU	Residue
SIGM2	Standard deviation of calculated diffusion coefficient
PFDD	Partial derivative of f_D with respect to D
ADELD	$\overline{\Delta D}$
G	L

Table V (continued)

Symbol	Meaning
D	D
T	Time, t
SUM	Xc_i
DERD	Analytical derivative of Xc_i with respect to D
SDERD	Second partial derivative Xc_i with respect to D
M	Mode control = 1 for first SUM calculation = 2 for all following SUM calculations
ALP	α
BET	β
XI	ξ
TAU	τ
Z(I)	λ_n where (I) corresponds to n

```
C     THIS PROGRAM PERFORMS A LEAST SQUARES ANALYSIS ON DIFFUSION DATA.

      MON$$     JOB  DATA ANALYSIS                                          J
      MON$$     COMT COMPILE,MISTLER NE DEPT, 10 PAGES, 15 MINUTES
      MON$$     ASGN MGO,16
      MON$$     ASGN MJB,12
      MON$$     MODE GO,TEST
S     MON$$     EXEO FORTRAN,,,12,,,,DATANAL
C      INPUT DATA ARE LISTED IN THE FOLLOWING ORDER--FIRST CARD,NSETS,
C        Z,R,V1,V2,ERR1 * SECOND CARD,ERR2 * THIRD CARD,NDATA, XLO, XDO,
C        AND ALL FOLLOWING CARDS,XEXP(K),T(K).  IF THERE ARE MORE THAN
C        ONE SET OF DATA THE THIRD CARD IS REPEATED AND THE DATA CARDS
C        ADDED.
C      ***NSETS=NO. OF SETS OF DATA          *** Z=DISTANCE VARIABLE
C      ***NDATA=NO. OF DATA POINTS IN SET    *** R=RADIUS OF TUBE
C      ***XLO=EFFECTIVE DIFFUSION LENGTH     *** V1=VOLUME OF FLASK 1
C      ***XDO=INITIAL GUESS OF D VALUE       *** V2=VOLUME OF FLASK 2
C      ***ERR1=ERROR CRITERION OF MAIN PROGRAM*** T(K)=TIME OF K DATA PT.
C      ***ERR2=ERROR CRITERION OF SUBPROGRAM
C      ***XEXP(K)=NORMALIZED ACTIVITY AT EACH K DATA PT.
       DIMENSION XEXP(40),T(40),XL(3),XD(3),XC(3,3,40),PXCD(40),PXCDD(40)
      B,XDIF(40)
       COMMON R,V1,V2,Z,ERR1,ERR2
     1 FORMAT(23H DIFFUSION COEFFICIENT=,E14.8)
     2 FORMAT(2F12.8)
     3 FORMAT(I5,5F15.7/E14.8)
     4 FORMAT(I5,2F15.7)
     5 FORMAT( 7H NSETS=,I5/5X,2HZ=,F10.4/5X,2HR=,F10.6/4X,3HV1=,F10.4/4X
      B,3HV2=,F10.4//7H  ERR1=,E14.8///6H  XLO=,F10.4/6H  XDO=,F10.4/7H ND
      CATA=,I5//18X,4HDATA,/6X,14HCONC. GRADIENT,7X,4HTIME)
     6 FORMAT(1H ,6X,F10.4,8X,F10.4)
     7 FORMAT(35H    ITERATION DIFFUSION COEFFICIENT=,E14.8)
     8 FORMAT(9H    ADELD=,E14.8)
     9 FORMAT(14H      RESIDUE =,E14.8)
    10 FORMAT(10X,1HT,13X,3HEXP,13X,2HXC)
    11 FORMAT(10X,F10.4,5X,F10.6,5X,F10.6)
    12 FORMAT(10X,12HSUM OF PXCD=,E14.8,5X,19HSUM OF SQRS OF PXCD,E14.8)
    13 FORMAT(10X,7HSIGMA =,E14.8)
    14 FORMAT(10X,7HSIGM2 =,E14.8)
       READ(1,3)NSETS,Z,R,V1,V2,ERR1,ERR2
       JSET=1
    15 READ(1,4)NDATA,XLO,XDO
       READ(1,2)(XEXP(K),T(K),K=1,NDATA)
       WRITE(3,5)NSETS,Z,R,V1,V2,ERR1,XLO,XDO,NDATA
    24 WRITE(3,6)(XEXP(K),T(K), K=1,NDATA)
C      THE VALUES NEEDED FOR THE SUBPROGRAM FOLLOW.
C         ***********
    25 XL(1)=XLO
       XD(1)=XDO
C          ***********
C      THE FOLLOWING CARD INITIALIZES THE SUBPROGRAM FOR THE FIRST XC.
C        CALCULATION
       CALL XCALF(0.,0.,0.,0.,0.,0.,1)
C      THIS SECTION CALCULATES THE PARTIAL DERIVATIVES OF XC.
```

```
C          ***********
      DO 20 J=1,NDATA
   20 CALL XCALF(XL(1),XD(1),T(J),XC(1,1,J),PXCD(J),PXCDD(J),2)
C          ***********
C      THIS SECTION EVALUATES THE DIFFERENCES BETWEEN EXPERIMENTAL AND
C        CALCULATED VALUES AND COMPUTES THE RESIDUES FOR EACH ITERATION.
C          ***********
      DO 50 J=1,NDATA
       XDIF(J)=XEXP(J)-XC(1,1,J)
   50 CONTINUE
      WRITE(3,10)
      WRITE(3,11)(T(J),XEXP(J),XC(1,1,J),J=1,NDATA)
      RSIDU=0.0
      DO 30 J=1,NDATA
   30 RSIDU=XDIF(J)**2 + RSIDU
      WRITE(3,9)RSIDU
C          ***********
C      THIS SECTION CALCULATES THE STANDARD DEVIATION, SIGM2.
C          ***********
      DPXCD=0.0
      SPXCD=0.0
      DO 31 J=1,NDATA
      DPXCD=PXCD(J)+DPXCD
   31 SPXCD=(PXCD(J)**2)+SPXCD
      WRITE(3,12)DPXCD,SPXCD
      DATA=NDATA
      SIGM2=SQRT(RSIDU/((DATA-1.0)*SPXCD))
      WRITE(3,14)SIGM2
C          ***********
C      THIS SECTION SUMS THE PARTIAL DERIVATIVES OF FD OVER ALL DATA
C        POINTS AND FINDS THE SUM OF THE FDC VALUES FOR EACH SET OF DATA.
C          ***********
      PFDD=0.0
      FDC=0.0
      DO 75   J=1,NDATA
      PFDD=(XDIF(J)*PXCDD(J)-PXCD(J)**2)+PFDD
       FDC=XDIF(J)*PXCD(J)+FDC
C          ***********
   75 CONTINUE
C      THIS SECTION CALCULATES THE DELTA D VALUE AND CHECKS TO SEE IF IT
C        IS SUFFICIENTLY SMALL. IF IT IS TOO LARGE ADELD IS ADDED TO D
C        AND ANOTHER ITERATION IS PERFORMED.WHEN IT IS SUFFICIENTLY SMALL
C        THE D CALCULATION TERMINATES AND ANOTHER SET OF DATA IS READ IN.
C          ***********
      ADELD=-FDC/PFDD
      WRITE(3,8)ADELD
      IF(ABS(ADELD/XDC).GT.ERR1)GO TO 150
  200 WRITE(3,1)XDC
      IF(JSET.LT.NSETS)GO TO 201
      GO TO 155
  201 JSET=JSET+1
      GO TO 15
  150 XDC=XDC+ADELD
      WRITE(3,7)XDC
      GO TO 25
C          ***********
```

```
  155 STOP
      END
S     MONS$      EXEQ FORTRAN,,,12,,,,XCALF

C     THIS SUBPROGRAM CALCULATES THE VALUE OF XC GIVEN L, D, AND T.

      SUBROUTINE XCALF(G,D,T,SUM,DERD,SDERD,M)
C     ***G=EFFECTIVE TUBE LENGTH      *** T=TIME
C     ***D=DIFFUSION COEFFICIENT      *** R=RADIUS OF CAPILLARY
C     ***SUM=XC                       *** S=DISTANCE VARIABLE Z
C     ***V1 AND V2= VOLUMES OF FLASKS
      DIMENSION Y(20),Z(20)
      COMMON R,V1,V2,S,ERR1,ERR2
   69 FORMAT(22X,13HXCALC VALUE =,E14.8)
      TANF(X)=SIN(X)/COS(X)
      SEC2F(X)=1./(COS(X)**2)
C     THE FOLLOWING SECTION SETS L,D, AND T EQUAL TO ZERO DURING THE
C       FIRST SUM CALCULATION FOR A SET OF INPUT DATA BUT RETAINS
C       PREVIOUS VALUES OF L,D, AND T DURING OTHER SUM CALCULATIONS.
C       THIS FACILITY IS PROVIDED TO HELP MINIMIZE THE NUMBER OF
C       SOLUTIONS TO THE TRANSCENDENTAL EQUATION.
C         ***********
      GO TO (5,6),M
    5 GS=0.
      DS=0.
      TS=0.
C         ***********
      RETURN
C     THIS SECTION EVALUATES ALPHA,BETA,XI,AND TAU AND DETERMINES
C       WHETHER OR NOT IT IS NECESSARY TO OBTAIN A SOLUTION TO THE
C       TRANSCENDENTAL EQUATION.  IF IT IS NOT NECESSARY, THE PROGRAM
C       PROCEEDS TO THE CALCULATION OF XC.  OTHERWISE, A NEW EIGENVALUE
C       IS CALCULATED.
C         ***********
    6 ALP=3.141592654*(R**2)*G/V1
      BET=(3.141592654*(R**2)*G)/V2
      C=ALP+BET
      Q=ALP*BET
      E=C+Q
      XI=S/G
      A=BET/(Q+C)
      TAU=T*D/(G**2)
      I=1
      SDERD=0.0
      DERD=0.0
      DERCK=0.0
      SUM=A
      IF(G.NE.GS) GO TO 270
      IF(D.NE.DS) GO TO 270
      GO TO 38
C         ***********
C     THE FOLLOWING SECTION CALCULATES THE SOLUTION TO THE TRANSCENDENTAL
C     EQUATION BY NEWTONS ITERATIVE METHOD.
C         ***********
  270 DO 999 I=2,20
  999 Y(I)=0.0
      Y(1)=-1.0
```

```
      I=1
  278 IF(Y(I))25,27,38
   25 Y(I)=E
      GO TO 200
   27 Z(I)=Z(I-1)+3.141592654
      GO TO 28
  200 Z(I)=SQRT(Y(I))
   28 X=Z(I)
      U=(Z(I)**2)-Q
      W=U**2
C     CARD 29 IS NEWTONS FORMULA APPLIED TO THE TRANSCENDENTAL EQUATION.
   29 Z(I)=X-(((W*TANF(Z(I)))-(U*C*Z(I)))/((U*(U*SEC2F(Z(I))-C))+(2.*Z(I
     B)**2*C)))
      Y(I)=Z(I)**2
      IF(ABS((1.-X/Z(I))).GT.ERR2) GO TO 28
C        ***********
C     THE FOLLOWING SECTION CALCULATES XC,DERD,AND SDERD USING THE
C       NUMBER OF TERMS NECESSARY TO SATISFY THE ERROR CRITERION. WHEN
C       ADDITIONAL EIGENVALUES ARE NEEDED THE CONTROL RETURNS TO THE
C       PRECEDING SECTION.
C         ***********
   38 H=SQRT(Y(I))
      CK=Y(I)*TAU.
      IF(CK-225.0)39,39,902
  902 TERM=0.0
      GO TO 42
   39 TERM=((1./(EXP(Y(I)*TAU)))*(H*COS(H)+(BET*SIN(H)))*((ALP*COS(H*XI)
     B)-(H*SIN(H*XI))))/(Y(I)*(((1./(2.*H))*(COS(H))*(C+Q-Y(I)))-((SIN(H
     C))*(1.+(.5*C)))))
C     DERD EQUALS THE FIRST DERIVATIVE OF XC WITH RESPECT TO D.
      DERD=(Y(I)*T/G**2)*TERM+DERD
      DERCK=SDERD
C     SDERD EQUALS THE SECOND DERIVATIVE OF XC WITH RESPECT TO D.
      SDERD=-((Y(I)*T/G**2)**2)*TERM+SDERD
   42 SUM=SUM-TERM
      IF(ABS(DERCK/SDERD).GT.ERR2)GO TO 44
      IF(ABS(TERM/SUM)-ERR2)47,47,44
   44 I=I+1
      GO TO 278
   47 GS=G
      DS=D
      TS=T
C        ***********
      RETURN
      END
S     MON$$      EXEQ LINKLOAD
                 CALL DATANAL
      MON$$      EXEQ DATANAL,MJB
```

RADIOACTIVE TRACER DETERMINATION OF GASEOUS DIFFUSION COEFFICIENTS

by

THOMAS ERIC MISTLER

B. S., Kansas State University, 1963

AN ABSTRACT OF A MASTER'S THESIS

submitted in partial fulfillment of the

requirements for the degree

MASTER OF SCIENCE

Department of Nuclear Engineering

KANSAS STATE UNIVERSITY
Manhattan, Kansas

1966

ABSTRACT

The purpose of this experimental study was to demonstrate the feasibility of using a modified Ney-Armistead diffusion cell to obtain reliable transition range diffusion coefficients for CO_2 at 20°C utilizing a radioactive tracer technique. Existing theory concerning gaseous diffusion in the bulk, Knudsen and transition pressure ranges was summarized. A survey was presented on the advantages and disadvantages of all existing methods for measuring diffusion coefficients. The properties and characteristics of semiconductor detectors were discussed to show their applicability to isotopic diffusion measurements in this type of diffusion apparatus. Considerable care was taken in presenting the apparatus and calculational procedures used to evaluate diffusion coefficients. A thorough analysis of the potential sources of experimental error was made and recommendations were presented for improving the system.

The diffusion apparatus used consisted of two flasks having volumes of 545 and 512 cc joined by a 0.1027 cm I. D. and 10.12 cm long capillary tube. The large flask contained a surface-barrier radiation detector. A solution to the one dimensional diffusion equation was derived for diffusion through this capillary tube using the effective diffusion length given by the Rayleigh correction factor. Least squares analysis was applied to obtain the diffusion coefficient measurement from the concentration versus time data. The use of a semiconductor detector was shown to combine the advantages of high counting efficiency and short time response to the convenience of internal detection of the tagged molecules. Diffusivity measurements on $C^{14}O_2$ demonstrated that this new apparatus can be used as a valuable research tool in the study of transition range diffusion.

Reported self-diffusion coefficients of CO_2 at 20°C between 50 and 400 microns agreed within 10 percent with the theory of Bosanquet and Wheeler for transition range diffusion. Measurements at pressures below 50 microns disagreed with theory by as much as 16 percent. The percentage error of the diffusion coefficients predicted by the residues of the least squares fit were approximately 3.5 percent at pressures between 50 and 400 microns while for lower pressures they were as high as 12 percent. These errors suggested the need for refinements in the capillary tube valve and the pressure measuring device.